

## Growth and demise of Cenozoic isolated carbonate platforms: New insights from the Mozambique Channel seamounts (SW Indian Ocean)

Courgeon Simon <sup>1,2,\*</sup>, Jorry Stephan <sup>2</sup>, Camoin G. F. <sup>1</sup>, Boudagher-Fadel M. K. <sup>3</sup>, Jouet Gwenael <sup>2</sup>, Revillon Sidonie <sup>4</sup>, Bachelery P. <sup>5</sup>, Pelleter Ewan <sup>2</sup>, Borgomano J. <sup>1</sup>, Poli E. <sup>6</sup>, Droxler A. W. <sup>7</sup>

<sup>1</sup> Aix Marseille Univ, CNRS, IRD, CEREGE UM34, F-13545 Aix En Provence, France.

<sup>2</sup> IFREMER, Inst Carnot Edrome, Unite Geosci Marines, F-29280 Plouzane, France.

<sup>3</sup> UCL, Earth Sci, 2 Taviton St, London WC1H 0BT, England.

<sup>4</sup> IUEM, Lab Domaines Ocean, SEDISOR UMR 6538, F-29280 Plouzane, France.

<sup>5</sup> Observ Phys Globe Clermont Ferrand, Lab Magmas & Volcans, 6 Ave Blaise Pascal, F-63178 Aubiere, France.

<sup>6</sup> CSTJF, TOTAL Explorat & Prod, Ave Larribau, F-64000 Pau, France.

<sup>7</sup> Rice Univ, Dept Earth Sci, Houston, DC 77005 USA.

\* Corresponding author : Simon Courgeon, email address : [simon.courgeon@gmail.com](mailto:simon.courgeon@gmail.com)

### Abstract :

Although long-term evolutions of isolated shallow-water carbonate platforms and demise episodes leading to guyot formation have been the subject of numerous studies during the last decades, their driving processes are still the subject of active debates. The Mozambique Channel (SW Indian Ocean) is characterized by several flat-topped seamounts ranging from 11°S to 21°S in latitudes. Based on a comprehensive geomorphologic study and on dredged samples analysis, we show that these features correspond to tropical isolated shallow-water carbonate platforms. Coupling strontium isotopy and foraminifera biostratigraphy, well-constrained chronostratigraphy results indicate that shallow-water carbonate production started in the Mozambique Channel during distinct Cenozoic periods ranging from Paleocene to Early Miocene. Our data also demonstrate that these carbonate platforms were subsequently characterized by different evolutions locally marked by tectonic and rejuvenated volcanism. While some of them kept developed until present days, forming modern carbonate systems, some others were drowned during Late Neogene and subsided to form guyots. Although different factors can be discussed, tectonic and volcanism appear as good potential triggers for demise episodes during Late Miocene-Early Pliocene times. Chronology and location of this geodynamical activity tend to emphasize influence of East African rift system until southern Mozambique Channel.

---

## Highlights

► The flat-top seamounts of the Mozambique Channel correspond to drowned isolated shallow-water carbonate platforms. ► Chrono-stratigraphy indicate that these carbonate systems colonized their substratum during distinct Cenozoic periods. ► Major backstepping and drowning episodes were most likely triggered by geodynamical activity (tectonic and volcanism). ► Mozambique Channel isolated carbonate platforms recorded southern and diffuse propagation of the East African rift system.

**Keywords** : Carbonate platform, Drowning, Cenozoic, Mozambique Channel, East African rift system

44

## 1. Introduction

45           Seamounts are presently defined as oceanic isolated positive topographic features  
46 either submarine, or sub-aerially exposed; their elevation is greater than 100m with respect to  
47 the surrounding seafloor (Wessel et al., 2010). They are essentially volcanic edifices formed  
48 by both intrusive and eruptive processes and located in oceanic intra-plate settings over  
49 upwelling mantle plumes, on- or off-axis mid-ocean ridges or along island-arcs (Staudigel and  
50 Clague, 2010). Guyots are seamounts that have built at or above sea level and whose flat top  
51 morphology is related to wave erosion (Staudigel and Clague, 2010). The top of guyots were  
52 once at the surface because they contain evidence of fossil shallow-water biological  
53 assemblages (e.g. Camoin et al., 1998).

54           During their geodynamic evolution, seamounts can reach the photic zone and be  
55 colonized by shallow-water carbonate builders (e.g. Hawaiian Islands; Moore and Clague,  
56 1992). Subsequent carbonate growth phases and seamount subsidence often lead to the  
57 formation of shallow-water isolated carbonate platforms (e.g. Pacific: Camoin et al., 1998;  
58 Wilson et al., 1998). While some of them have survived and aggraded until present-day to  
59 form modern isolated carbonate platforms (e.g. Enewetak and Pikinni atolls; Wilson et al.,  
60 1998), many of them were subsequently drowned, forming „guyots“ (or tablemounts; Camoin  
61 et al., 1998). Many interactive factors are considered to explain platform drowning, including  
62 (1) an abrupt increase in accommodation space outpacing carbonate growth potential and  
63 flooding the shallow-water carbonate platform below the photic zone (e.g. Schlager, 1981;  
64 Toomey et al., 2013), (2) a sharp decrease in carbonate factory production related to the  
65 degradation of environmental and climatic conditions, including subaerial exposure (e.g.  
66 Schlager, 1998) and excess of clastic and/or nutrient input (e.g. Hallock and Schlager, 1986;  
67 Camoin et al., 1998; Wilson et al., 1998; Schlager, 1999; Betzler et al., 2009), and (3) long

68 term geodynamical processes, such as dynamic subsidence (e.g. Schlager, 1999; DiCaprio et  
69 al., 2010). Under stress, the surface area of the factory may often shrink and retreat towards  
70 more elevated or more protected topographies to overcome inimical environmental conditions  
71 or to keep pace with the rapid increase in accommodation space. In this situation, the  
72 drowning of the carbonate system is therefore only partial and is recorded by typical  
73 backstepping morphologies (e.g. Schlager, 2005).

74         The growth and demise of isolated carbonate platform are common in the geological  
75 record (e.g. Camoin et al., 1998; Wilson et al, 1998) but the processes involved on time scales  
76 of tens of millions years have been barely determined and quantified (Schlager et al, 1999). A  
77 great diversity of isolated carbonate platforms initiated and developed during Cenozoic times  
78 in the Indo-Pacific realm. In the Maldives, shallow-water carbonate production was initiated  
79 during the Eocene when shallow-water carbonate banks were formed (Aubert and Droxler,  
80 1992). Subsequent depositional sequences were characterized by multiple carbonate growth  
81 phases separated by periods of sub-aerial exposure and drowning events driven either by  
82 eustatic sea-level changes (Purdy and Bertram, 1993; Beloposky and Droxler, 2004), bottom  
83 current activity (Lüdmann et al, 2013) or Indian Monsoon activity (Betzler et al., 2009). On  
84 Limalok guyot, occurring at 1255m deep in the Pacific Ocean, the shallow-water carbonate  
85 production was initiated during the Late Paleocene on a volcanic substrate and the subsequent  
86 carbonate platform development, including periods of sub-aerial exposure, ended with its  
87 drowning during middle Eocene times (Ogg et al., 1995). Drowning events affecting late  
88 Cretaceous and early Cenozoic Pacific guyots are thought to be related to the motion of the  
89 Pacific plate that displaced shallow-water carbonate platforms into low-latitude, inimical  
90 environmental conditions (Wilson et al., 1998). The large diversity of geological processes  
91 which control the development and the drowning of Cenozoic isolated carbonate platforms  
92 illustrates the sensitivity of such systems to changes in accommodation space and

93 environmental conditions on relatively long time scales. New case studies improve our  
94 understanding of shallow-water isolated carbonate systems.

95         The Mozambique Channel (MC) is located in the SW Indian Ocean, between the  
96 eastern African margin and Madagascar, and is characterized by several and distinct modern  
97 isolated carbonate systems forming the “Iles Eparses”. In addition to these islands, low-  
98 resolution GEBCO bathymetrical grids indicate that, in the MC, several seamounts and guyots  
99 currently occur hundreds of meters deep and are good potential analogues of classic drowned  
100 carbonate platforms. Based on new data collected during oceanographic cruises carried out in  
101 2014, this work aims at: (1) investigating the morphology and the nature of the flanks of  
102 modern isolated systems and surrounding flat-top seamounts, (2) determining the ages of  
103 major episodes of shallow-water carbonate production and comparing them to the records of  
104 other isolated carbonate platforms from the Indo-Pacific oceans and, (3) discuss timing and  
105 processes of shallow-water carbonate platforms demise and (4) describing isolated platform  
106 geodynamic specificities and replacing the seamounts in the MC regional context.

## 107 **2. Geological Setting**

108         The MC is a broad, almost triangular, trough bounded by the Mozambique continental  
109 slope to the west and the Madagascar continental slope to the east (Fig. 1A & 1B). The  
110 formation of the MC modern structure is related both to the break-up of the Gondwana Super-  
111 Continent which occurred during the Early Jurassic-Early Cretaceous time span, and to the  
112 relative drifting between the African and “Antarctico-Indio-Madagascarian” continental  
113 blocks (Coffin and Rabinowitz, 1987). This main structuration phase was followed by  
114 stabilization and tectonic\volcanic stages as, for instance, during the separation of India and  
115 Antarctica from Madagascar around 84 Ma (Bassias, 1992), or more recently, with tectonic  
116 activity linked to the onset and development of the East African rift system (EARS) from the

117 Oligocene up to present days (Salman and Abdula, 1995, Chorowicz, 2005, McGregor, 2015,  
118 Fig. 2).

119         The southward motion of Madagascar relative to Africa occurred from the Middle  
120 Jurassic to the Early Cretaceous (~165-120 Ma) through the activity of a major transform  
121 fault known as “Davie Ridge” (DR, e.g. Coffin and Rabinowitz, 1987; Fig. 1B & 2). This  
122 fracture zone currently corresponds to a NNW-SSE bathymetrical high of ~1200 km in width  
123 and crossing longitudinally the MC (Fig. 1B). The DR is made of crystalline continental  
124 basement consisting of gneiss and meta-arkose, covered in places by alkaline lava, tuff and  
125 breccias and by a thin layer of Cretaceous to modern carbonate oozes (Leclaire et al., 1989;  
126 Bassias, 1992). The DR hosts several prominent submarine morphologies including, from  
127 north to south, the Saint Lazarus, Paisley, Macua and the Sakalaves seamounts whose nature  
128 and morphology remain poorly known. The south central part of the MC is characterized by a  
129 cluster of seamounts including the Hall and the Jaguar banks, the Bassas da India atoll and the  
130 Europa platform (Fig. 1B & 1C). Although the origin of these seamounts is seemingly related  
131 to oceanic volcanism, no dredging has been carried out in that region to confirm this  
132 hypothesis. The Sakalaves and southern MC seamounts (i.e. Bassas da India, Hall and Jaguar  
133 banks) are located in a diffuse zone of the southern EARS (Kusky et al., 2010; Rovuma plate,  
134 Calais et al., 2006) between the Nubian and African plates (Fig. 2).

135         The northernmost part of the MC hosts the Comoro Archipelago (Fig. 1B) which is  
136 composed of four volcanic islands, from West to East: Grande Comore, Mohély, Anjouan and  
137 Mayotte. Geochronological data indicate a diachronous magmatic activity, from about 20 Ma  
138 in Mayotte to present-day in Grande Comore (Emerick and Duncan, 1982; Michon, 2016).  
139 The origin of this archipelago is still debated and could correspond either to a deep mantle  
140 plume developing a hotspot track or, conversely, to a lithospheric deformation that reactivated  
141 transform faults and controlled the magma path (Michon, 2016). To the Northwest, the

142 Glorieuses carbonate platform, the northernmost Iles Eparses, may also have developed on a  
143 volcanic edifice linked to this regional trend (Emerick and Duncan, 1982).

144 Nowadays, the modern isolated carbonate platforms forming the Iles Eparses are small  
145 and flat coral platforms. Covering a total of 44 sq. km with a highest elevation which does not  
146 exceed a few meters, the shallow-marine carbonate production typically reflects tropical  
147 neritic productivity dominated by corals, large benthic foraminifera (LBF), green algae, and  
148 molluscs (Battistini, 1976; Jorry et al., 2016; Prat et al., 2016). Last interglacial reefs form  
149 localized outcrops, which are affected by karstic processes (presence of plurimeter dissolution  
150 cavities), more or less colonized by vegetation.

### 151 **3. Material and Methods**

152 This work is mainly based on geophysical and geological data acquired during the  
153 2014 PTOLEMEE and PAMELA-MOZ1 cruises onboard the RV *L'Atalante*, as part of the  
154 PAMELA (Passive Margin Exploration Laboratory) research project. Geological  
155 interpretations presented in this study result from the combined analysis of (1) bathymetry  
156 DEMs and associated slope maps, (2) rock samples, and (3) underwater videos.

157 Bathymetric data were acquired with Kongsberg EM122 (Frequency of 12kHz) and  
158 Kongsberg EM 710 (Frequency from 71 to 100kHz) multibeam systems. Data were processed  
159 using CARAIBES<sup>TM</sup> v4.2 software and were respectively gridded into 10m and 5m resolution  
160 DEMs (WGS84). Geomorphological and morphometric analysis, as well as slope maps, were  
161 processed with ArcGIS<sup>TM</sup> v10.3 using customized Mercator<sup>TM</sup> projections. Analysis and  
162 geological interpretation were supported by 3D visualization with Fledermaus<sup>TM</sup> v7 system.  
163 We also used laser bathymetry and topography (LiDAR) grids acquired between 2009 and  
164 2011 by the Litto3D program to illustrate the modern geomorphology of the Iles Eparses.

165 Underwater videos and associated pictures were collected through an interactive,  
166 submarine camera system (SCAMPI) developed by IFREMER. Viewing, analyzing and geo-  
167 referencing of the videos were carried out with the ADELI<sup>TM</sup> Video v3-beta system  
168 (Ifremer©). Rock samples were collected using Niwa (DNxx - samples) and Warren (DWxx -  
169 samples) dredges on flat surfaces capping the seamounts, and using rock dredges (DRxx -  
170 samples) along the flanks of the seamounts.

171 The sedimentological interpretation combines hand sample and thin section  
172 observations. The reconstruction of carbonate depositional environments is based on the  
173 interpretation of biological assemblages and depositional textures. In our definitions of  
174 stratigraphic ranges, we primarily use the planktonic foraminifer zonal scheme described by  
175 BouDagher-Fadel (2015), which is tied to the timescale defined by Gradstein et al. (2012).  
176 We also used previous benthic and foraminiferal zonal scheme from BouDagher-Fadel (2008;  
177 2013).

178 Some limestone samples were dated using Sr Isotope Stratigraphy (SIS; McArthur,  
179 2012). To avoid bias in measured  $^{87}\text{Sr}/^{86}\text{Sr}$  ratios related to post depositional processes, we  
180 adopted a sequential dissolution method using weak acetic acid prior to Sr separation using  
181 Eichrom® Sr spec Resin (Pin and Santos Zalduegui, 1997). Sr isotope compositions were  
182 measured in static mode on a Thermo TRITON at the PSO (“Pôle de Spectrométrie Océan”)  
183 in Brest, France. All measured ratios were normalized to  $^{86}\text{Sr}/^{88}\text{Sr} = 0.1194$  and NBS987  
184 (recommended value 0.710250). Ages were obtained using the LOWESS fit 4babacuses of  
185 McArthur (2012). Uncertainties on ages were calculated by combining the external  
186 reproducibility on measured  $^{87}\text{Sr}/^{86}\text{Sr}$  ratios with uncertainties on the LOWESS fit  
187 mathematical model. Detailed values of SIS analysis are presented in additional data online  
188 (see supplementary 1).

## 189 **4. Results**

### 190 **4.1. General geomorphology of the Mozambique Channel flat top seamounts**

191 The southern part of the MC is characterized by a SW-NE trending irregular ridge  
192 morphology supporting three flat top seamounts (Fig. 1C): the Bassas da India atoll (Fig. 3A),  
193 the Hall Bank (Fig.4A) and the Jaguar Bank (Fig. 5A). This ridge is characterized by crater  
194 and cones morphologies (Fig. 3A, 3B & 5A) that suggest a volcanic origin.

195 Bassas da India (Fig. 3A) is a roughly circular atoll of about 10 km in diameter and 80  
196 sq.km. The width of the reef rim averages 100 m and completely encloses a shallow lagoon  
197 which displays a maximum depth of 15 m. The southern flank of the modern atoll of Bassas  
198 da India is typified by a 12km-wide flat top morphology (B1, Fig. 3A & 3C). The bathymetry  
199 of this terrace ranges from -680m to -440m and is bounded by two linear escarpments, 50 to  
200 200m high, extending towards the seabed (>1500m water-depth). These escarpments are  
201 seemingly associated to major normal faults inducing important vertical offsets of terraces. A  
202 minor and shallower flat top level can be observed around 220m deep (B2, Fig. 3A & 3C).  
203 The Hall Bank (Fig. 4) averages 90 sq.km.in areal extent and is characterized by two terraces  
204 (H1 & H2, Fig. 4A & 4E). The most prominent level is the shallowest one (H2) which occurs  
205 between 430m and 525m while the secondary and deepest one (H1) is located at 600m water  
206 depth. The Jaguar Bank (Fig. 5) is located 20km west of the Hall Bank (Fig. 1C) and covers  
207 an area of 320 sq.km approximately. This seamount also exhibits an overall flat-topped  
208 morphology but is characterized by an extensive, high escarpments network (Fig. 5A). These  
209 lineaments, interpreted as normal faults, seemingly structure the overall morphology of the  
210 Jaguar Bank (Fig. 5C). They limit several tilted panels ranging from 700m to 170m deep on  
211 the northern margin and on the summit (southern extremity, Fig. 5A & 5C) respectively.  
212 Bassas da India, the Hall and Jaguar banks flat-topped submarine morphologies exhibit sharp

213 and abrupt margins that are commonly incised by well-developed, 0.5 to 4.5 km wide, steep  
214 convex bankward embayments (Fig. 3A, 4A & 5A). The most important embayment is  
215 located on the northeastern flank of Bassas da India, and seems responsible for the “notched”  
216 morphology of the modern atoll (Fig. 3A).

217         The DR is typified by an overall flat top morphology of 275 sq.km known as the  
218 “Sakalaves Seamount” (Fig. 1B & 6A) which is located at about 18° S, in the middle of the  
219 MC. This platform morphology extends over a distance of 30 km from north to south and over  
220 12km from west to east, and is characterized by an elongated shape following the NNW-SSE  
221 orientation of the DR (Fig. 6A). The Sakalaves Platform is affected by numerous linear  
222 escarpments displaying the same trend, and dividing the overall morphology into multiple flat  
223 top levels ranging from 500m (overall platform margin) to 335m (NW and SE extremities)  
224 deep (Fig. 6A & 6C). These escarpments exhibit typical characteristics of normal faults on  
225 bathymetrical data (Fig. 6C). To the west, a shallower level is characterized by its very rugged  
226 morphology (“ru”, Fig. 6A). The abrupt slopes of the seamount are also incised by well-  
227 developed truncation embayment morphologies, especially along its western flank (Fig. 6A).

228         The Glorieuses carbonate platform (Fig. 1B & 7A) is located about 160km northwest  
229 of Madagascar. It displays SW-NE and SE-NW extensions respectively of more than 20 km  
230 and of 17 km (Fig. 7A), and covers an area of about 230 sq.km. This platform includes an  
231 archipelago comprised of a group of islands and rocks covering 5 sq.km. The flanks of the  
232 Glorieuses platform and the nearby areas are characterized by several flat-topped  
233 morphologies and associated slope breaks (Fig. 7A) ranging from 1100m (G1) to 200m (G3)  
234 water depths. The NNW flank of the Glorieuses platform exhibits a drowned terrace around  
235 750m deep (G2, Fig. 7). The latter is incised by a 2.5 km wide embayment. All these flat-  
236 topped terraces are located on a rough submarine ridge, the top of which occurs at -1000 m  
237 water depth, northwest of the Glorieuses Platform.

## 239 **4.2. Surface morphologies**

240 The coupled analysis of high-resolution bathymetry grids (Fig. 3B, 4B, 4C, 4D, 5B,  
241 6B & 7B) and underwater videos (Fig. 8) were used to determine the nature of geological  
242 features. The flanks of the drowned platforms are characterized by flat, smooth and bright  
243 rocky slabs (e.g. Hall Bank and Glorieuses, Fig. 8A & 8B respectively) that are frequently  
244 characterized by thin and regular networks of fractures; these formations display common  
245 characteristics of carbonate rocks. Along the northeastern flank of the Hall Bank, the slope  
246 between the two main terraces (i.e.. H1 and H2, Fig. 4A) is characterized by smaller-scale,  
247 successive and parallel terrace morphologies that typify backstepped margins (Fig. 4D).  
248 Except for the Glorieuses, the MC drowned flat-topped morphologies are also characterized  
249 by well-developed closed to semi-enclosed circular depressions (e.g. Fig. 4A & 6B) that are  
250 tens of meters to 1300m wide and up to 40m deep.

251 With the exception of the Glorieuses, the tops of the overall flat top morphologies are  
252 characterized by a great diversity of rugged and positive morphologies that seemingly  
253 intersect and partially cover the previous flat-topped topographies (Fig. 3, 4, 5 & 6). The very  
254 rugged flat top level located on the western side of the Sakalaves Platform (“ru.”, Fig. 6B)  
255 exhibits a dense network of 50 to 2000m long, and 10 to 30m wide linear positive ridges.  
256 Although these ridges mostly display a regional NNW-SSE trend, they commonly form  
257 polygonal patterns and irregular heaps. Rugged morphologies and irregular reliefs are also  
258 observed on top of the Bassas da India terrace level (B1, Fig. 3A & 3C), as well as on top of  
259 Hall (Fig. 4) and Jaguar Banks (Fig. 5). Underwater pictures made along these morphologies  
260 (Fig. 8D, 8E & 8F) illustrated outcrops of very dark rocks associated both with rounded rocky  
261 formations resembling pillow-lavas, and dense polygonal fracturing networks that are similar

262 to the tensional/contraction cracks that typically develop during submarine volcanic eruptions  
263 (e.g. Yamagishi, 1991; Chadwick et al., 2013). On top of the Jaguar Bank, some of these  
264 rugged morphologies exhibit lobate and interdigitated downslope-flowing morphologies (Fig.  
265 5B) displaying striking similarities with submarine lobate lava flows (see Gregg and Fink,  
266 1995). Underwater pictures taken on the western part of the Sakalaves platform top (ru level,  
267 Fig. 6A) show dark intrusions into brighter rocky outcrops (Fig. 8C), suggesting that the ridge  
268 network (Fig. 6B) corresponds to eroded volcanic dyke system.

### 269 **4.3. Dredged samples**

270 Rock samples collected along rough ridges (Dredges DR -04, -13, -17 & -19, see  
271 respective locations Fig. 1C, 6A & 7A) on which platform morphologies are established  
272 correspond to blocks of volcanic rocks (pictures available in additional data online; see  
273 supplementary 2). They are mostly composed of alkali mafic lavas (olivine basalts to  
274 nephelinites) at Bassas da India, Hall Bank, Jaguar Bank, and Sakalaves Platform. Rock  
275 samples collected on the NW ridge of the Glorieuses include encrusted trachy-andesite to  
276 trachyte lava. Polygenic pebbles that have been collected at the top of the Hall Bank (DW05,  
277 see location on Fig 4A) are composed of altered volcanic material (lavas and volcanic  
278 breccias; see additional data available online for illustrations) and limestones. These pebbles  
279 are systematically encrusted by very dark Fe-Mn oxyhydroxides layers that are up to 7mm  
280 thick. Overall, rock samples collected on the upper flanks and at the top of drowned flat-  
281 topped morphologies are limestones (Fig. 9, Tab. 1).

282 Rock sample collected along the SW flank of the Hall Bank (DR18-01, see location on  
283 Fig. 4A) corresponds to a skeletal packstone bearing large corals grains encrusted by red algae  
284 and encrusting foraminifera, many robust LBF as well as *Halimeda* algae (Fig. 9A, 9B & 9C;  
285 Table 1). Such biological composition typically reflects tropical shallow-water depositional

286 settings. The microfauna assemblage is characterized by *Miogypsina regularia* (Fig. 9C) and  
287 *Lepidocyclina brouweri* (Fig. 9B) which corresponds to N8a planktonic foraminifera zone  
288 (Burdigalian, BouDagher-Fadel, 2008; 2015). The isotopic strontium stratigraphy (SIS)  
289 indicates a consistent age of 16.29 +/- 0.10 Ma (Tab. 1; detailed SIS values are presented in  
290 supplementary 1 online). In addition to volcanic pebbles and undated highly altered corallgal  
291 limestones, the top of the Hall Bank (DW05; Fig. 4A) is characterized by the occurrence of a  
292 planktonic foraminifera packstone (DW5-C1, Fig. 9D, Tab. 1) typifying an outer neritic  
293 environment. It includes *Sphaeroidinella dehiscens* (Fig. 9D), *Globorotalia tumida*,  
294 *Globigerinoides quadrilobatus* (Fig. 9D) as well as common *Globigerina* spp. and  
295 *Globorotalia* spp; this assemblage corresponds to N18-N19 planktonic foraminifera zone  
296 defined by BouDagher-Fadel, 2015 (Late Messinian - Early Zanclean, 5.8-3.8 Ma), in  
297 agreement with the Zanclean age given by the isotopic strontium stratigraphy (i.e. 5.09 Ma,  
298 Tab. 1).

299 Rock sample collected along the southeastern flank of Bassas da India (DR20-01, see  
300 location on Fig. 3A) corresponds to a skeletal packstone mainly comprised of planktonic  
301 foraminifera, encrusting foraminifera and coral fragments, red algae and bivalves (Fig. 9E &  
302 9F, Tab. 1). The microfauna assemblage includes *Orbulina suturalis* (Fig. 9E), *Orbulina*  
303 *universa*, *Globoquadrina dehiscens* as well as *Dentoglobigerina altispira* and corresponds to  
304 the N9-N20a planktonic foraminifera zone (Middle Miocene - Early Pliocene). SIS gives a  
305 consistent late Miocene age of 8.48 +/- 0.49 Ma (Tortonian, Tab. 1).

306 Dredgings carried out along the eastern flank of the Sakalaves Platform (DR13, see  
307 location on Fig. 5A) recovered volcanic rocks and limestones which correspond to a LBF-rich  
308 grainstone typified by rhodoliths and volcanic fragments (DR13-08; Fig. 9G & 9H, Tab. 1).  
309 These limestones include *Spiroclypeus vermicularis* (Fig. 9C) and *Cycloclypeus koolhoveni*,  
310 which can be attributed to the P18-P19 foraminifera zones (BouDagher-Fadel, 2013; 2015,

311 Rupelian, 33.9-30.3 Ma, Tab. 1). The obtained SIS age is of 33.11 +/- 0.14 Ma (Early  
312 Oligocene, Rupelian) for DR13-08 and is therefore consistent with biostratigraphic data. Rock  
313 samples recovered from the top of the Sakalaves Platform (DW04, see location on Fig.6A) are  
314 comprised of corallgal boundstone (DW04-01, Fig. 9I) and outer shelf planktonic foraminifera  
315 packstone (DW04-02a, Fig. 9J). The occurrence of *Cycloclypeus postinornatus* and  
316 *Cycloclypeus carpenteri* in DW04-01 indicates the N14 to N21 shallow benthic zones  
317 (BouDagher-Fadel, 2008; 2015, Late Miocene-Pliocene, 11.6-1.8 Ma). SIS gives an age of  
318 8.80 +/- 0.35 Ma (Tortonian) for DW04-01 (Fig. 9). DW04-02a includes *Sphaeroidinella*  
319 *subdehiscens*, *Globoquadrina* sp. and *Orbulina universa* (Fig. 9J) and is associated to N19-  
320 N20 planktonic foraminifera zone (Zanclean; BouDagher-Fadel, 2015; Tab. 1). For the latter,  
321 no SIS age is available.

322 Finally, rock samples collected on the flat top morphology located NW of the  
323 Glorieuses (DN01, see location on Fig. 6J) correspond to corallgal boundstones with pockets  
324 of Discocyclinid LBF packstones (Fig. 9K & 9L). The relevant assemblage, characteristic of a  
325 tropical shallow-water depositional environment, includes *Discocyclina sella* (Fig. 9L) and  
326 *Daviesina* sp. and coincides with the P3-P5a foraminifera zone (BouDagher-Fadel, 2008,  
327 Paleocene). SIS analysis on DN01-01 provides three potential ages of 67.11 +/-0.27 Ma,  
328 61.52 +/- 1.80 Ma and 33.89 +/- 0.15 Ma. The foraminifera assemblage indicates that this  
329 limestone is Selandian to Thanetian in age (Paleocene), thus suggesting that the correct SIS  
330 age is of 61.52 +/- 1.80 Ma (Tab. 1).

## 331 **5. Discussion**

### 332 **5.1. Origin of Mozambique Channel flat top seamounts**

333 While most of flat top seamounts are currently drowned at hundreds of meters deep  
334 (i.e below the photic zone), the MC submarine plateaus and terraces display typical

335 geomorphological features of shallow-water carbonate platforms. Their morphologies are  
336 characterized by successive very steep margins delineating distinct terraces levels (Fig. 3, 4,  
337 5, 6 & 7) that are interpreted as resulting from different phases of carbonate platform  
338 development and backstepping. The observed very steep margins, characterized by bright  
339 rocky slabs (Fig. 8A & 8B), are very reminiscent of shallow-water carbonate flanks that  
340 typically accumulate along tropical carbonate platforms. The biological assemblages that  
341 characterize the limestones samples recovered along MC carbonate platforms are mainly  
342 composed of hermatypic corals, coralline red algae, green algae (*Halimeda*) and LBF (Fig. 9),  
343 thus confirming a tropical shallow-water depositional environment. The combination of  
344 biostratigraphic and strontium isotopic data demonstrates that MC shallow-water carbonate  
345 platforms colonized their volcanic substrates during distinct Cenozoic time windows, ranging  
346 from the Paleocene to the Early Miocene.

347 The rounded depressions (Fig. 4A & 6B) observed on top of the drowned terraces of the south  
348 MC and Sakalaves flat-top seamounts could be related to explosive events or gravity collapses  
349 associated to volcanic activity (e.g. Chadwick et al., 2013). They might also correspond to  
350 karst pits caused by carbonate dissolution processes and associated collapses (e.g. Grigg et al.,  
351 2002; Guidry et al., 2007) into a carbonate platform which underwent (a) long period(s) of  
352 subaerial exposure. As observed along numerous ancient and modern carbonate platforms  
353 margins (e.g. Bahamas Archipelago, Jo et al., 2015), the MC drowned platform margins are  
354 incised by well-developed steep convex-bankward embayments (mfs, Fig 3A, 4A, 5A, 6A &  
355 7B). These truncation features, also called "scalped margins" (Mullins and Hine, 1989) are  
356 interpreted as erosional features resulting from catastrophic large-scale margin failures  
357 usually induced by earthquake shocks in tectonically active areas, and by dissolution  
358 processes and/or deep water currents in stable regions (Mullins and Hine, 1989; Jo et al.,  
359 2015).

360 **5.2. Long-term (Paleocene to Present) evolution of the Glorieuses carbonate**  
361 **platform**

362 In the northern part of the MC channel, the Glorieuses volcanic ridge (Fig. 7A) was  
363 colonized by an isolated carbonate system during the Paleocene (Fig. 10) at the latest, as  
364 indicated by the Selandian to Thanetian age (Tab. 1) of its second terrace level (G2, Fig. 7B)  
365 which crops out at 750m deep. The coralgall limestones that are associated with abundant  
366 Discocylinid LBF suggest that this drowned terrace developed in a shallow-water  
367 depositional environment. Although Early Paleogene platform carbonates are often poorly  
368 preserved and/or inaccessible (Baceta et al., 2005), LBF-rich reef carbonates have been well  
369 documented in Paleocene shallow-water formations (e.g. Bryan, 1991; Scheibner and Speijer,  
370 2008b). The occurrence of a carbonate terrace (G1, Fig 7A), at approximately 1100m deep,  
371 suggests that carbonate production started even before the Late Paleocene, i.e. most likely  
372 during Early Paleocene or Late Cretaceous. Overall, the distinct terrace levels (G1, G2 & G3;  
373 Fig. 7) observed along the flanks of the Glorieuses carbonate platform are interpreted as  
374 resulting from successive development and backstepping episodes, before the initiation of  
375 modern shallow-water carbonate systems.

376 The drowning of the 750m deep coralgall Paleocene terrace (G2, Fig. 7B) could be  
377 associated with the major long-term climatic warming of the Paleocene-Eocene transition  
378 during which many Tethyan coral reef systems declined (Scheibner and Speijer, 2008a,b).  
379 Furthermore, the narrowness of the volcanic ridge which is located NW of the Glorieuses  
380 platform potentially deprived the carbonate builders of an appropriate large substrate on  
381 which the platform could have backstepped. Despite the occurrence of successive terraces  
382 (Fig. 7), the long-term evolution of the Glorieuses carbonate platform appears relatively  
383 continuous at the Cenozoic time scale. The development of shallow-water carbonate

384 platforms during the Cenozoic is quite common in the Western Indian Ocean, as indicated for  
385 instance at de Saya de Malha and Nazareth Banks (Mascareign Ridge), where exploration  
386 wells SM1 and NB-1 (Texaco Inc.) have penetrated Late Paleocene to Pliocene shallow-water  
387 carbonate platform limestones (Kamen-Kaye and Meyerhoff, 1980).

### 388 **5.3. Oligo-Miocene growth of south MC and Sakalaves shallow-water carbonate** 389 **platforms**

390 The shallow-water carbonate production on the Sakalaves Platform, presently drowned  
391 at 335 m deep, was initiated on the DR during the Oligocene (Tab. 1, Fig. 10). The occurrence  
392 of many volcanic fragments (Fig. 9G) into the skeletal packstone recovered along the western  
393 flank of the Sakalaves platform suggests the presence of nearby volcanic reliefs during  
394 carbonate deposition, confirming that the colonization occurred during Rupelian time. The  
395 LBF and red algae-rich carbonate assemblage that characterizes the relevant carbonates (Fig.  
396 9G & 9H, Tab. 1) is quite similar to that of other Oligocene shallow-water carbonate  
397 platforms, such as the *Lepidocyclina* limestones that have been described in early Oligocene  
398 deposits of the Cayman Brac isolated carbonate bank (Caribbean, Jones and Hunter, 1994).  
399 Drilling operations carried out on the Kerendan platform (Oligocene, Indonesia) also reported  
400 packstones that are rich in large benthic foraminifera and fragments of coralline algae (Saller  
401 and Vijaya, 2002). The Sakalaves carbonate platform most likely continued its development  
402 during Miocene times (Fig. 10) until the deposition of Late Miocene (Tortonian) corallgal  
403 frameworks (Fig. 6A & 9I). This result is consistent with a previous study reporting Miocene  
404 limestones on top of the platform (Leclaire et al., 1989). The presence of Zanclean outer shelf  
405 packstones suggests that the drowning of the Sakalaves shallow-water carbonate platform  
406 occurred during Late Miocene to Early Pliocene times (Fig. 10)

407 In the South MC, the analysis of limestone samples collected along the southwestern  
408 flank of the Hall Bank (Tab. 1) suggests that carbonate production started at the latest during  
409 the Early Miocene (Fig. 10). Although no Early Miocene carbonate samples have been  
410 collected along the flanks of Bassas da India and of the Jaguar Bank, these features are  
411 located on the same volcanic ridge and presently occur at similar depths (i.e. 600-800m, Fig.  
412 3, 4 & 5), thus suggesting that they may have appeared during the same period. The  
413 abundance of encrusted coral fragments, robust large benthic foraminifera and *Halimeda*  
414 algae (DR18-01 & DR20-01; Tab. 1) indicates that the South MC Miocene limestones were  
415 deposited in shallow-water carbonate environments. Similar Miocene carbonate assemblages  
416 have been commonly reported in the Indo-Pacific realm and were often associated to reef  
417 systems (e.g. Australia, Betzler and Chapronière, 1993; Bornéo, Wilson, 2005; Indonesia,  
418 Novak et al., 2013). During its evolution, the Hall Bank underwent a major backstepping  
419 episode which shifted carbonate production from H1 to H2 terrace (Fig. 4A & 4D). The  
420 demise of shallow-water carbonate sedimentation on the Hall Bank is marked by the  
421 deposition of outer shelf carbonates during early Pliocene times (Tab. 1, Fig. 10). Conversely,  
422 in Bassas da India, aggradation processes continued until present days to form a modern atoll.  
423 The Fe-Mn crusts observed on pebbles collected on top of the Hall Bank have been  
424 commonly reported on top of drowned shallow-water carbonate platforms (e.g. Pacific  
425 guyots, Bogdanov et al., 1995; Camoin et al., 1998) where they have been interpreted as  
426 resulting from a slow precipitation onto hard substrates in areas swept by strong bottom  
427 current (e.g. Mangini et al., 1986).

428 **5.4. Late Miocene - Early Pliocene drowning phases: tectonic and rejuvenated**  
429 **volcanism as major triggers ?**

430 The occurrence of extensive volcanic morphologies (Fig. 3, 4 & 5) and material, and  
431 of widespread faults and fracturing networks on tops of drowned carbonate terraces suggest  
432 that geodynamic activity could be involved in shallow-water carbonate platforms demises  
433 during Late Miocene to Early Pliocene times. Morphological analysis as well as underwater  
434 pictures and dredge samples display many evidences of subaqueous extrusive volcanism (e.g.  
435 pillow lavas and lobate lava flow, Fig. 4C, 5B, 8D, 8E & 8F) but also of intrusive volcanism  
436 especially typified by dyke morphologies as observed along the Sakalaves Platform (Fig. 6B  
437 & 8C). Relevant eruptive phases brought volcanic material (e.g. lava flow, volcanoclasts) and  
438 significant environmental changes (e.g. water transparency, water temperature) that likely  
439 stressed and smothered shallow-dwelling carbonate producers. In parallel, The MC drowned  
440 carbonate platforms are affected by widespread and extensive faults and fracturing networks  
441 which display extensional deformation patterns such as frequent high-offset normal faults  
442 (e.g. Fig. 3, 5A, 5C & 6). In this context, drowning of the MC shallow-water carbonate  
443 platforms could be related to extensional deformation and rapid pulses of tectonic subsidence  
444 outpacing carbonate accumulation rates. For instance, the occurrence of two high-offsets  
445 normal faults delimiting Bassas da India first terrace (B1, Fig. 3A) suggests that tectonic  
446 movements were involved in the major backstepping phase through the sudden drowning of  
447 shallow-water carbonate producers below the photic zone. The continuous development of  
448 Bassas da India isolated carbonate systems after late Miocene-Pliocene drowning events  
449 suggests the occurrence of topographic highs, such as tectonically raised area, that  
450 subsequently allowed the backstepping of the shallow-water carbonate factory. Volcanic  
451 morphologies (e.g. lava deltas, Hawaii; Puga-Bernabéu et al., 2016) may be also colonized by  
452 shallow-water carbonate systems during backstepping processes in response to a rapid  
453 increase in accommodation space or to environmental deterioration. Along Tonasa carbonate  
454 platform (Sulawesi, Indonesia), Wilson (2000) also described shallow-water carbonate

455 platform evolution and demise that were primarily controlled by tectonic and volcanic  
456 activity.

457 Environmental disturbances (e.g. nutrient input, paleo-climatic and -oceanographic changes)  
458 are frequently invoked to explain the demise of shallow-water carbonate platform and also  
459 have to be discussed. Dredge samples analysis suggest that demise of the Sakalaves Platform  
460 and drowning episodes of south MC carbonate platforms took place during late Miocene to  
461 early Pliocene times (Fig. 10). In the Indo-Pacific realm, several drowning episodes induced  
462 by environmental deterioration have reported during the same Neogene time span. On the  
463 Marion Plateau (Australia), cooling and re-organization of ocean circulation triggered during  
464 Late Miocene, successive drowning events of the carbonate platform (Eberli et al., 2010).  
465 Along Maldives carbonate platform, Betzler et al. (2009) proposed that late Miocene-Early  
466 Pliocene partial drowning of the platform is linked to onset and intensification of the  
467 Monsoon trough injection of nutrient into shallow-water. Coeval drowning episodes in the  
468 Indo-Pacific realm suggest that environmental conditions deterioration linked to paleo-  
469 climatic and paleo-oceanographic reorganization could also be involved in Late Neogene  
470 demise of the MC shallow-water carbonate platforms. Finally, the rounded depressions  
471 observed on Hall Bank top and that potentially correspond to karst pits, might suggest  
472 extended periods of subaerial exposure which are potential triggers of major drowning events  
473 (e.g. Schlager et al., 1998).

## 474 **5.5. Geodynamical implications**

475 Two primary conditions are required for the initiation and development of a tropical  
476 isolated carbonate system: (1) the existence of a hard substrate available for the settlement of  
477 shallow-water carbonate producers, and (2) the occurrence of such a substrate in the euphotic  
478 zone. This study demonstrated that the MC carbonate platforms developed on irregular and

479 isolated volcanic reliefs (Fig. 1C, 3, 5 & 7; rock samples pictures available on supplementary  
480 2 online). In the Glorieuses, the record of a Selandian to Thanetian terrace (G2, Fig. 7 & Tab.  
481 1) implies that the volcanic event that was responsible for the formation of the seamount  
482 occurred before the Late Paleocene (Fig. 10). This volcanic phase could be related to the  
483 interaction between Madagascar and the Marion Hotspot (Meert and Tamart, 2006) and to the  
484 coeval breakup of Madagascar and Greater India during late Cretaceous times (Storey et al.,  
485 1995). The Glorieuses seamount may belong to a SE-NW volcanic axis running from  
486 northwestern Madagascar coast towards Aldabra Atoll and encompassing the Leven Bank  
487 (Fig. 2). The minimum Paleocene age of the Glorieuses seamount seemingly excludes its links  
488 with the volcanic activity recorded in the Comoros Archipelago and that has been recently  
489 interpreted as resulting from a lithospheric deformation in relation to the East African Rifting  
490 during late Cenozoic times (Michon, 2016, Bachélery and Hémond, 2016). With the  
491 exception of the G2 terrace, the Glorieuses platform does not exhibit evidences of major  
492 drowning events during its Cenozoic development. In parallel, no evidence of tectonic or of  
493 any renewed volcanic activity has been observed along its flank and in the nearby areas  
494 suggesting that the Glorieuses carbonate platform has evolved in an overall stable  
495 geodynamical setting since Early Paleogene times. Taking into account that Paleocene  
496 eustatic sea level was approximately 50m above present day sea level (Miller et al., 2005), the  
497 average subsidence of the Glorieuses seamount since the Paleocene is estimated between 10  
498 and 15m/Myr.

499         Based on volcanic substrates, south MC and Sakalaves drowned carbonate platforms  
500 display striking evidences of volcanic and tectonic activities during and/or after carbonate  
501 platform development. In the southern MC, the eruptive phases responsible for the  
502 development of a volcanic ridge (Fig. 1C) probably occurred during Oligocene to early  
503 Miocene times, before its colonization by isolated carbonate systems and subsequent

504 development of carbonate platforms during the Miocene (Fig. 10). A phase of rejuvenated  
505 volcanism and tectonic deformation took place in the Middle Miocene to Pliocene time span,  
506 and possibly until the Pleistocene (Fig. 10). Along the DR, on the Sakalaves Platform, the  
507 combination of geomorphological analysis and the dating of carbonate samples also  
508 demonstrate that tectonic deformation and volcanism occurred from the Oligocene to the  
509 present days. The Sakalaves Platform, which is affected by a dense fault network parallel to  
510 NNW-SSE DR trend, is located in a seismically active area which seemingly corresponds to  
511 an extension of the EARS offshore branch (McGregor, 2015; Fig. 2). The large margin failure  
512 scars incising carbonate platform slopes (Fig. 3, 4, 5 & 6) could also indicate a sustained  
513 tectonic activity (e.g. Mullins and Hine, 1989) along MC Cenozoic carbonate platforms. The  
514 volcanic and extensional tectonic phases that have been identified along the Sakalaves  
515 Platform and in the southern Mozambique Channel are coeval with the activity of the EARS  
516 during Cenozoic times (McGregor, 2015), i.e. from Oligocene to present-day. Moreover, the  
517 Sakalaves and southern MC carbonate platforms are located in a diffuse zone of the EARS  
518 (Kusky, 2010) between Nubian and Somalian plates (Fig. 2). This area has been also  
519 interpreted as another plate (Rovuma plate; Calais et al., 2006) and is characterized by  
520 scattered but significant modern seismicity (Fig. 2). The formation of the volcanic basement  
521 which forms the substrate of some MC carbonate platforms, as well as the extensional  
522 tectonic and rejuvenated volcanism observed at the top of the platforms are thus interpreted as  
523 links to EARS development and tend to confirm its southern diffuse propagation (Kusky,  
524 2010). This example illustrates again that isolated shallow-water carbonate production has the  
525 ability to record regional-scale geodynamic activity but also, conversely, that geodynamical  
526 processes appear as major control parameters of tens of millions year shallow-water carbonate  
527 platform evolution (e.g. Wilson, 2000; Yubo et al., 2011).

## 528 **6. Conclusions**

529 The main results of this study can be summarized as follow:

530 (1) The flat top and drowned seamounts of the Mozambique Channel correspond to  
531 ancient tropical and isolated shallow-water carbonate platforms that initially settled on  
532 volcanic substrates.

533 (2) The Mozambique Channel isolated carbonate platforms, located in different  
534 geodynamical settings, set on during distinct Cenozoic periods ranging from Paleocene to  
535 Early Miocene. These chronostratigraphic results are consistent with important phases of  
536 shallow-water carbonate platform growth in the Indo-Pacific realm during the Cenozoic.

537 (3) The Mozambique Channel isolated carbonate platforms underwent distinct  
538 polyphase evolutions that locally comprised tectonic deformation, volcanism and major  
539 backstepping and drowning phases. Although the origin of demise episodes remain unclear,  
540 tectonic and rejuvenated volcanism appear as most likely triggers. In parallel, Glorieuses and  
541 Bassas da India shallow-water carbonate platforms survived and kept on developing until  
542 present-day.

543 (4) Along the Sakalaves and the south Mozambique Channel carbonate platforms,  
544 Cenozoic tectonic and volcanic activity is coeval and seems spatially linked to the  
545 development and the propagation of the Eastern African rift system. The Paleocene onset of  
546 shallow-water carbonate production at the Glorieuses carbonate platforms suggest Late  
547 Mesozoic volcanism north of Madagascar, decoupled from more recent EARS activity.

548 Processes controlling shallow-water carbonate platform growth and demise on time  
549 scales of tens of millions year periods are actively discussed but they remain poorly mastered.  
550 The MC, representing a new promising area to study shallow-water carbonate platforms  
551 growth and drowning events, suffers from lack of coring data to quantify numerous crucial  
552 parameters such as growth rates or high frequencies environmental fluctuations. In this

553 context, drilling operations along the MC channels flat-top seamounts would offer an  
554 outstanding opportunity to improve our understanding of isolated shallow-water carbonate  
555 platforms systems.

556

## 557 **Acknowledgements**

558 We are grateful to Captain, Officers, and crew members of the 2014 PTOLEMEE  
559 (<http://dx.doi.org/10.17600/14000900>) and PAMELA-MOZ1  
560 (<http://dx.doi.org/10.17600/14001000>) cruises onboard the R/V *L'Atalante* for their technical  
561 support in recovering high-quality dataset. We thank Stephane Bodin and an anonymous  
562 reviewer for insightful comments on the previous version of this manuscript. The authors  
563 warmly thank Philippe Fernagu (Ifremer) for the preparation of thin-sections and Charline  
564 Guérin, Arnaud Gaillot and Delphine Pierre for bathymetry grids processing. The  
565 oceanographic expeditions PTOLEMEE and PAMELA-MOZ1 as well as the Mozambique  
566 2014 study were co-funded by TOTAL and IFREMER as part of the PAMELA (Passive  
567 Margin Exploration Laboratory) scientific project.

568

## 569 **References**

- 570 Aubert, O., Droxler, A.W., 1992. General Cenozoic evolution of the Maldives carbonate system (equatorial  
571 Indian Ocean). Bulletin Des Centres de Recherches Exploration-Production Elf-Aquitaine 16, 113-136.  
572
- 573 Baceta, J.I., Pujatte, V., Bernaola, G., 2005. Paleocene corallgal reefs of the western Pyrenean basin, northern  
574 Spain: New evidences supporting an earliest Paleogene recovery of reefal ecosystems. Palaeogeography,  
575 Palaeoclimatology, Palaeoecology 224, 117-143  
576
- 577 Bachèlery, P., Hémond, C., 2016. Geochemical and Petrological Aspects of Karthala Volcano, in Active  
578 volcanoes of the Southwest Indian Ocean, in Active volcanoes of the world, Bachèlery, P., Lénat, J.-F., Di Muro,  
579 A., Michon, L. (Eds.), 2016, Springer-Verlag, Chapter 23, 367-384  
580
- 581 Bassias, Y., 1992. Petrological and geochemical investigation of rocks from the Davie Fracture Zone  
582 (Mozambique Channel) and some tectonic implications. Journal of African Earth Sciences 15, 321-339.  
583
- 584 Battistini R., Gayet J., Jouannic C., Labracherie M., Peypouquet J.P., Pujol C., Pujos-Lamy A., Turon J.L.  
585 (1976) Etude des sédiments et de la microfaune des îles Glorieuses (Canal du Mozambique). Cah. ORSTOM  
586 Ser. Géol. 2, 147-171.  
587

- 588 Belopolsky, A.V., Droxler, A.W., 2004. Seismic expressions and interpretations of carbonate sequences: The  
589 Maldives carbonate platform, equatorial Indian Ocean. *American Association of Petroleum Geologists Studies in*  
590 *Geology* 49, 46 p.
- 591
- 592 Betzler, C., Brachert, T.C., Kroon, D., 1995. Role of climate in partial drowning of the Queensland Plateau  
593 carbonate platform (northeastern Australia). *Marine Geology* 123, 11-32.
- 594
- 595 Betzler, C., Chaproniere, G.C.H., 1993. Paleogene and Neogene larger foraminifers from the Queensland  
596 Plateau: biostratigraphy and environmental significance. *Proceedings of Ocean Drilling Programs, Scientific*  
597 *results* 133, p 51-66.
- 598
- 599 Betzler, C., Hübscher C., Lindhorst, S., Reijmer, J.J.G., Römer, M., Droxler, A.W., Fürstenau, J., Lüdmann, T.,  
600 2009. Monsoon-induced partial carbonate platform drowning (Maldives, Indian Ocean). *Geology* 39, 867-870.
- 601
- 602 Bogdanov, Y.A., Bogdanova, O.Y., Dubinin, A.V., Gorand, A., Gorshkov, A.I., Gurvich, E.G., Isaeva, A.B.,  
603 Ivanov, G.V., Jansa, L.F., Monaco, A., 1995. Composition of ferromanganese crusts and nodules at northwestern  
604 Pacific guyots and geologic and paleoceanographic considerations, in: Haggerty, J.A., Premoli Silva, I., Rack,  
605 F., and McNutt, M.K. (Eds.), *Proceedings of the Ocean Drilling Program, Scientific Results* 144, 745-768.
- 606
- 607 BouDagher-Fadel, M.K., 2015. *Biostratigraphic and Geological Significance of Planktonic Foraminifera*,  
608 London, UCL Press, 298 p.
- 609
- 610 BouDagher-Fadel, M.K., 2013. Diagnostic First and Last Occurrences of Mesozoic and Cenozoic Planktonic  
611 Foraminifera. *Professional Papers Series*, 1-4.
- 612
- 613 BouDagher-Fadel, M.K., 2008. Evolution and Geological Significance of Larger Benthic Foraminifera.  
*Developments in Palaeontology and Stratigraphy* 21, 1-548.
- 614
- 615 Bryan, J. R. 1991. A Paleocene coral-algal-sponge reef from southwestern Alabama and the ecology of Early  
616 Tertiary reefs. *Lethaia* 24, 423-438.
- 617
- 618 Calais, E., Ebinger, C., Hartnady, C., Nocquet, J.M., 2006. Kinematics of the eastern African Rift from GPS and  
619 earthquake slip vector data. *Geological society of London special publications* 259, 9-22.
- 620
- 621 Camoin, G.F., Arnaud-Vanneau, A., Bergersen, D.D., Enos, P., Ebren, P., 1998. Development and demise of  
622 mid-oceanic carbonate platforms, Wodejato Guyot (NW Pacific). *International Association of*  
*Sedimentologists Special Publication* 25, 39-67.
- 623
- 624 Chadwick Jr., W.W., Clague, D.A., Embley, R.W., Perfit, M.R., Butterfield, D.A., Caress, D.W., Paduan, J.B.,  
625 Martin, J.F., Sasnett, P., Merle, S.G., Bobbitt, A.M., 2013. The 1998 eruption of Axial Seamount: New insight  
626 on submarine lava flow emplacement from high-resolution mapping. *Geochemistry, Geophysics, Geosystems*  
14, 3939-3968.
- 627
- 628 Chorowicz, J., 2005. The East African rift system. *Journal of African Earth Sciences* 43, 379-410.
- 629
- 630 Coffin, M. F., Rabinowitz, P. D., 1987. Reconstruction of Madagascar and Africa: evidence from the Davies  
631 Fracture Zone and Western Somali Basin. *Journal of Geophysical Research* 92, 9385-9406.
- 632
- 633 DiCaprio, L., Dietmar Müller, R., Gurnis, M., 2010. A dynamic process for drowning carbonate reefs on the  
634 northeastern Australian margin. *Geology* 38, 11-14.
- 635
- 636 Eberli, G.P., Anselmetti, F.S., Isern, A.R. & Delius, H., 2010. Timing of changes in sea-level and currents along  
637 Miocene Platforms on the Marion Plateau, Australia. In: *Cenozoic Carbonate Systems of Australia* (Ed. by  
638 Morgan W.A., George A.D., Harris P.M., J.A. Kupezec & J.F. Sarg), *SEPM Spec. Publ.* 95, 219-242. SEPM,  
Tulsa, OK.
- 639
- 640 Emerick, C.M., Duncan, R.A., 1982. Age progressive volcanism in the Comores Archipelago, western Indian  
Ocean and implications for Somali plate tectonics. *Earth and Planetary Science Letters* 60, 415-428.
- 641
- 642 Gradstein, F.M., Ogg, J.G., Hilgen, F.J., 2012. On the Geologic Time Scale. *Newsletters on Stratigraphy* 45,  
171-188.

- 641 Gregg, T.K.P., Fink, J.H., 1995. Quantification of submarine lava-flow morphology through analog experiments.  
642 *Geology* 23, 73-76.
- 643 Grigg, R.W., Grossman, E.E., Earle, S.A., Gittings, S.R., Lott, D., McDonough, J., 2002. Drowned reefs and  
644 antecedent karst topography, Au'au Channel, S.E. Hawaiian Islands. *Coral Reefs* 21, 73-82.
- 645 Guidry, S.A., Grasmueck, M., Carpenter, D.G., Gombos, Jr., A.M., Bachtel, S.L., Viggiano, D.A., 2007. Karst  
646 and early fracture networks in carbonates, Turks and Caicos Islands, British West Indies. *Journal of Sedimentary  
647 Research* 77, 508-524.
- 648 Hallock, P., and Schlager, W., 1986. Nutrient excess and the demise of coral reefs and carbonate platforms.  
649 *Palaios* 1, 389-398.
- 650 Jo, A., Eberli, G.P., Grasmueck, M., 2015. Margin collapse and slope failure along southwestern Great Bahama  
651 Bank. *Sedimentary Geology* 317, 43-52. *Facies* 30, 25-50.
- 652 Jones, B., Hunter, I.G., 1994. Evolution of an isolated carbonate bank during Oligocene, Miocene and Pliocene  
653 times, Cayman Brac, British Western Indies.
- 654 Jorry, S.J., Camoin, G.F., Jouet, G., Le Roy, P., Vella, C., Courgeon, S., Prat, S., Paumard, V., Boule, J., Caline,  
655 B. and Borgomano, J., 2016. Modern sediments and Pleistocene reefs from isolated carbonate platforms (Iles  
656 Eparses, SW Indian Ocean): A preliminary study. *Acta Oecologica* 72, 129-143.
- 657 Kamen-Kaye, M., Meyerhoff, A.A., 1980, Petroleum geology of the Mascarene Ridge, Western Indian Ocean.  
658 *Journal of Petroleum Geology* 3, 123-138.
- 659 Kusky, T.M., Toraman, E., Raharimahefa, T., Rasoazanamparany, C., 2010. Active tectonics of the Alaotra-  
660 Ankay Graben system, Madagascar: Possible extension of Somalian-African diffuse plate boundary. *Gondwana  
661 Research* 18, 274-294.
- 662 Leclaire, L., Bassias, Y., Clocchiatti, M. and Segoufin, J., 1989. La formation de la ride de Davie. Approche  
663 stratigraphique et géodynamique. *Comptes Rendus de l'Académie des Sciences de Paris* 308, 1077-1082.
- 664 Lüdmann, T., Kalvelage, C., Betzler, C., Fürstenau, J., Hübscher, C., 2013. The Maldives, a giant isolated  
665 carbonate platform dominated by bottom currents. *Marine and Petroleum Geology* 43, 326-340.
- 666 Mangini, A., Halbach, P., Puteanus, D., Segl, M., 1987 Chemistry and growth history of central Pacific Mn  
667 crusts and their economic importance, *Marine Minerals*, 205-220.
- 668 McArthur, J. M., Howarth, R. J. et al., 2012. Chapter 7 - Strontium Isotope Stratigraphy. *The Geologic Time  
669 Scale 2012*, Boston, Elsevier, 127-144.
- 670 McGregor, D., 2015. History of the development of the East African Rift System: A series of interpreted maps  
671 through time. *Journal of African Earth Sciences* 101, 232-252.
- 672 Moore, J.G., Clague, D.A., 1992. Volcano growth and evolution of the island of Hawaii. *Geological Society of  
673 America Bulletin* 104, 1471-1484.
- 674 Michon, L., 2016. The volcanism of the Comoros Archipelago integrated at a regional Scale, in: Bachelery, P.,  
675 Lénat, J.-F., Di Muro, A., Michon, L. (Eds.), *Active volcanoes of the Southwest Indian Ocean*. Springer-Verlag,  
676 the Netherlands 333-344.
- 677 Miller, K.G., Kominz, M.A., Browning, J.V., Wright, J.D., Mountain, G.S., Katz, M.E., Sugarman, P.J., Cramer,  
678 B.S., Christie-Blick, N., & Pekar, S.F., 2005. The Phanerozoic record of global sea-level change. *Science* 310,  
679 1293-1298.
- 680 Meert, J.G., Tamrat, E., 2006. Paleomagnetic evidence for a stationary Marion hotspot: Additional  
681 paleomagnetic data from Madagascar. *Gondwana Research* 10, 340-348.
- 682 Mullins, H.T., Hine, A.C., 1989, Scalloped bank margins; beginning of the end for carbonate platforms?  
683 *Geology* 17, 30-33.  
684

- 685 Novak, V., Santodomingo, N., Rösler, A., Di Martino, E., Braga, J.C., Taylor, P.D., Renema, W., 2013.  
686 Environmental reconstruction of a late Burdigalian (Miocene) patch reef in deltaic deposits (East Kalimantan,  
687 Indonesia). *Palaeogeography, Palaeoclimatology, Palaeoecology* 374, 110-122  
688
- 689 Ogg, J.G., Camoi, G.F., Arnaud Vanneau, A., 1995. LimalokGuyot: depositional history of the carbonate  
690 platform from downhole logs at site 871 (lagoon), in: Haggerty, J.A., Premoli Silva, I., Rack, F., and McNutt,  
691 M.K. (Eds.), *Proceedings of the Ocean Drilling Program, Scientific Result 144*, 233-253.  
692
- 693 Pin, C., Santos Zalduegui, J.F., 1997. Sequential separation of light rare-earth elements, thorium and uranium by  
694 miniaturized extraction chromatography: Application to isotopic analyses of silicate rocks. *Analytica Chimica*  
695 *Acta* 339, 79-89.
- 696 Prat S., Jorry S.J., Jouet G., Camoin G.F., Vella C., Le Roy P., Caline B., Boichard R., Pastol Y. (2016)  
697 Geomorphology and sedimentology of a modern isolated carbonate platform: The glorieuses archipelago, SW  
698 Indian Ocean. *Marine Geology*, in press
- 699 Puga-Bernabéu, A., Webster, J.M., Braga, J.C., Clague, D.A., Dutton, A., Eggins, S., Fallon, S., Jacobsen, G.,  
700 Paduan, J.B., Potts, D.C., 2016. Morphology and evolution of drowned carbonate terraces during the last two  
701 interglacial cycles, off Hilo, NE Hawaii. *Marine Geology* 371, 57-81.
- 702 Purdy, E.G., Bertram, G.T., 1993. Carbonate concepts from the Maldives, Indian Ocean: American Association  
703 of Petroleum Geologists *Studies in Geology*, v. 34, 56 p..
- 704 Saller, A.H., Vijaya, S., 2002. Depositional and diagenetic history of the Keredan carbonate platform, Oligocene,  
705 Central Kalimantan, Indonesia. *Journal of Petroleum Geology* 25, 123-150.
- 706 Salman, G., Abdula, I., 1995. Development of the Mozambique and Ruvuma sedimentary basins, offshore  
707 Mozambique, *Sedimentary Geology* 96, 7-41.
- 708 Scheibner, C., Speijer, R.P., 2008a. Decline of coral reefs during late Paleocene to early Eocene global warming.  
709 *eEarth* 3, 19-26.
- 710 Scheibner, C., Speijer, R.P., 2008b. Late Paleocene-early Eocene Tethyan carbonate platform evolution - A  
711 response to long- and short-term paleoclimatic change, *Earth-Science Reviews* 90, 71-102.
- 712 Schlager, W., 1981. The paradox of drowned reefs and carbonate platforms. *Geological Society of America*  
713 *Bulletin* 92, 197-211.
- 714 Schlager, W., 1998. Exposure, drowning and Sequence Boundaries on Carbonate platforms, in *Reefs and*  
715 *Carbonate Platforms in the Pacific and Indian Oceans*, Camoin, G.F., Davies, P.J. (Eds.), *Special Publications of*  
716 *International Association of Sedimentologists* 25, 3-21.
- 717 Schlager, W., 1999. Scaling of sedimentation rates and drowning of reefs and carbonate platforms. *Geology* 27,  
718 p. 183-186
- 719 Schlager, W., 2005. *Carbonate Sedimentology and Sequence Stratigraphy*. SEPM Concepts in Sedimentology  
720 and Paleontology, Series no. 8, 200 p.
- 721 Staudigel, H., Clague, D.A., 2010. The geological history of deep-sea volcanoes: Biosphere, hydrosphere, and  
722 lithosphere interactions. *Oceanography* 23, 58-71.
- 723 Toomey, M., Ashton, A.D., Perron, J.T., 2013. Profiles of ocean islands coral reefs controlled by sea-level  
724 history and carbonate accumulation rates. *Geology* 41, 731-734.
- 725 Wessel, P., Sandwell, D.T., Kim, S.S., 2010. The global seamount census, *Oceanography* 23, 24-33.
- 726 Wilson, M.E.J., 2000. Tectonic and volcanic influences on the development and Diachronous termination of a  
727 Tertiary tropical carbonate platform. *Journal of Sedimentary Research* 70, 310-324.
- 728 Wilson, M.E.J., 2005. Development of equatorial delta-front patch reefs during the Neogene, Borneo. *Journal of*  
729 *Sedimentary Research* 75, 114-133.

730 Wilson, P.A., Jenkyns, H.C., Elderfield, H., Larson, R.L., 1998. The paradox of drowned carbonate platforms  
731 and the origin of Cretaceous Pacific guyots. *Nature* 392, 889- 894.  
732  
733 Yamagishi, H., 1991. Morphological and sedimentological characteristics of the Neogene submarine coherent  
734 lavas and hyaloclastites in Southwest Hokkaido, Japan, *Sedimentary Geology* 74, 5-23.  
735  
736 Yubo, M., Shiguo, W., Fuliang, L., Dongdong, D., Qiliang, S., Yintao, L., Mingfeng, G., 2011. Seismic  
737 characteristics and development of the Xisha carbonate platforms, northern margin of the South China Sea.  
738 *Journal of Asian Earth Sciences* 40, 770-783.  
739

## 740 **Captions**

741 **Figure1:** (A) Location of the Mozambique Channel in the Western Indian Ocean (B) General  
742 physiography of the Mozambique Channel, bathymetry grid comes from GEBCO (100m  
743 resolution, 2008). Studied seamounts are in bold.(C) Detailed physiography of Southern  
744 Mozambique Channel seamounts, red line and lettering correspond to dredging. Isobaths have  
745 been computed every 500m water depth.

746 **Figure2:** The Mozambique Channel and the East African rift system. Glo means Glorieuses  
747 Platform. The Sakalaves Platform (Sa) and south MC carbonate platform (Ba) are located in a  
748 diffuse zone of the EARS (Kusky et al., 2010). This area between western and southeastern  
749 branches is also interpreted as another plate: the Rovuma plate (Calais et al., 2006). The two  
750 white lines drawn north of Madagascar represent an hypothetical Late Mesozoic volcanic  
751 alignment (see details in the text). Elevation/bathymetry grid comes from GEBCO (100m  
752 resolution).

753 **Figure3:** (A) Geomorphology of Bassas da India Atoll seamount (see location on figure 1B &  
754 1C). Green italic lettering corresponds to the nomenclature for successive flat-topped features  
755 interpreted as drowned carbonate terraces and platforms. Red lines and lettering correspond to  
756 dredgings. White boxe corresponds to the location of specific geomorphologies shown in  
757 figure 3B. The yellow star corresponds to a sea bottom picture presented in figure 8. Black  
758 dashed lines and lettering correspond to the location of morphological cross-sections shown in  
759 figure 3C. fe: fault escarpments; mfs: margin failure scar. (B) Close up of volcanic cones

760 morphology (C) Morphological cross-sections of Bassas da India terraces. The red star  
761 corresponds to the approximate location of DR20 dredge along morphological cross-section.

762 **Figure4:** (A) Overall geomorphology of the Hall Bank seamount (see location on figure 1B &  
763 1C). Green italic lettering corresponds to the nomenclature for successive flat-topped features  
764 interpreted as drowned carbonate terraces and platforms. Red lines and lettering correspond to  
765 dredgings. White boxes correspond to the location of specific geomorphologies shown in  
766 figure 4B, 4C & 4D. The yellow star corresponds to a submarine picture shown in figure 8.  
767 Black dashed lines and lettering correspond to the location of morphological cross-sections  
768 shown in figure 4E. fe: fault escarpment; mfs: margin failure scar.(B) Close up of rounded  
769 depressions interpreted as resulting from volcanic or karstic processes. (C) Close up of  
770 rugged, positive features along the H2 drowned carbonate terrace. This morphology is  
771 interpreted as resulting from submarine volcanic eruptions. The yellow star corresponds to an  
772 underwater picture shown in figure 8. (D) Close up of backstepping features interpreted as  
773 successive "backstepped" carbonate terraces. (E) Morphological cross-sections of Hall Bank  
774 margins. The red star corresponds to the approximate location of DR18 dredge along  
775 morphological cross-section.

776 **Figure5:** (A) Overall geomorphology of the Jaguar Bank seamount (see location on figure 1B  
777 & 1C). The red box corresponds to the location of a specific morphologies shown in figure  
778 5B. fe: fault escarpment; mfs: margin failure scar. This overall flat-topped feature, interpreted  
779 as a drowned carbonate platform, is characterized by a dense normal fault network delimiting  
780 several tilted blocs. Black dashed line and lettering correspond to the location of the  
781 morphological cross-section shown in figure 5C (B) Close up of a positive, rough and lobate,  
782 morphology interpreted as a submarine lava flow (see text for more details). (C)  
783 Morphological cross-sections of the Jaguar Bank.

784 **Figure6:** (A) Overall geomorphology of the Sakalaves Platform (see location on figure 1B)  
785 interpreted as a drowned shallow-water carbonate platform. Red lines and lettering  
786 correspond to dredge sampling. ru. in green italic lettering locates a flat-topped level  
787 characterized by very rugged reliefs. The white box corresponds to the location of a specific  
788 morphology shown in figure 6B. Black dashed line and lettering correspond to the location of  
789 the morphological cross-section shown in figure 6C. fe: fault escarpment; mfs: margin failure  
790 scar (B) Close up of the very rough flat topped level located on the western part of the  
791 Sakalaves Platform. These dense network comprised of linear positive ridges and surrounding  
792 heaps is interpreted as an eroded volcanic dyke system (for more details see the text).The  
793 yellow stars correspond to the location of underwater pictures shown in figure 8. (C)  
794 Morphological cross-sections of the Sakalaves Platform. The red star corresponds to the  
795 approximate location of DW04 dredge along morphological cross-section.

796 **Figure7:**(A) Overall geomorphology of the Glorieuses platform (see location on figure 1B).  
797 Green italic lettering corresponds to the nomenclature for successive flat-topped features  
798 interpreted as drowned carbonate terraces and platforms. No fault nor recent volcanic features  
799 are observed. The white box corresponds to the location of a specific morphology shown in  
800 figure 7B. mfs: margin failure scar.(B) Close up of the drowned carbonate platform G2 which  
801 occurs at 750m deep, northwest of the modern Glorieuses Platform. Red lines and lettering  
802 correspond to the location of dredgings. The yellow star corresponds to the location of sea  
803 bottom pictures shown in figure 8.

804 **Figure8:**Sea bottom pictures. (A) Limestone slab along the northern flank of the Hall Bank  
805 (see location on figure 3A). (B) Limestone slab along the G2 drowned carbonate terrace,  
806 northwest of the Glorieuses Platform (see location on figure 7B). (C) Volcanic dyke at the top  
807 of the Sakalaves Platform (see location on figure 6B). (D) Pillow lavas at the top of the  
808 Sakalaves Platform (see location on figure 6B).(E) Very dark volcanic outcrops with well-

809 developed fracturing network at the top of the Hall Bank (H2, see location on figure 4C).(F)  
810 Lobate submarine lava flow on top of the B1 drowned carbonate terrace (Bassas da India, see  
811 location on figure 3A).

812 **Figure9:** Thin sections micrographs. RA: Rodophyte Algae; Co: Coral; Ha: Halimeda algae;  
813 EF: Encrusting Foraminifera, Ech: Echinoids. DR18-01 (A, B, C): Burdigalian skeletal  
814 packstone with encrusted coral grains, *Lepidocyclina brouweri* Rutten (Lb) and *Miogypsina*  
815 *regularia* BouDagher-Fadel and Price (Mio). DW05-C1 (D): Late Messinian - Early Zanclean  
816 packstone of planktonic foraminifera typified by *Sphaeroidinella dehiscens* Parker and Jones  
817 (Sa), *Globigerinoides quadrilobatus* d'Orbigny (Gdes) and *Globoquadrina dehiscens*  
818 Chapman, Parr, and Collins (Gq). DR20-01 (E,F): Middle Miocene - Early Pliocene skeletal  
819 Packstone characterized by *Cycloclypeus carpenteri* Brady (Cc) and *Orbulina suturalis*  
820 d'Orbigny (Os). DR18-03 (G, H): Rupelian skeletal packstone of LBF with volcanic  
821 fragments (v); *Lepidocyclina* sp. (L), *Daviesina* sp. (Da) and *Spiroclypeus vermicularis* Tan  
822 Sin Hok (Sv). DW04-01 (I): Coralgal Boundstone. DW04-02 (J): Zanclean packstone of  
823 planktonic foraminifera typified by *Sphaeroidinella subdehiscens* Parker and Jones (Ss),  
824 *Globoquadrina* sp. and *Orbulina universa* d'Orbignyi (Ou). DN01 (K, L): Coralgal  
825 Boundstone with pockets of LBF packstones typified by *Discocyclina sella* d'Archiac (Di).

826 **Figure10:** Timing of major phases of shallow-water carbonate platform development and  
827 geodynamic activity along Mozambique channels seamounts during Cenozoic times.

828 **Table1:** : Table summarizing dating results, depositional textures, main composition and  
829 interpreted depositional environments of carbonate samples described and used in this study.

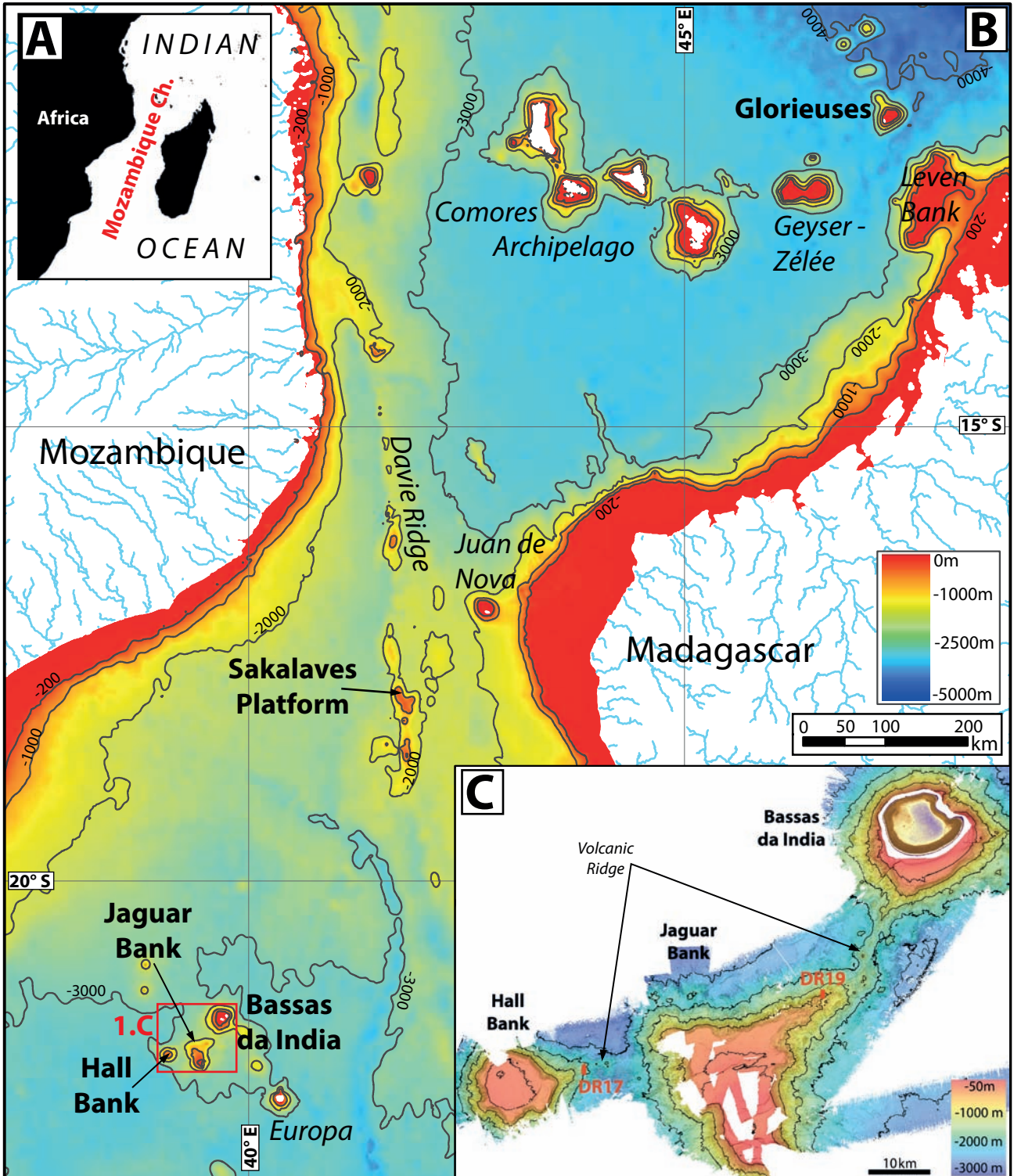
830

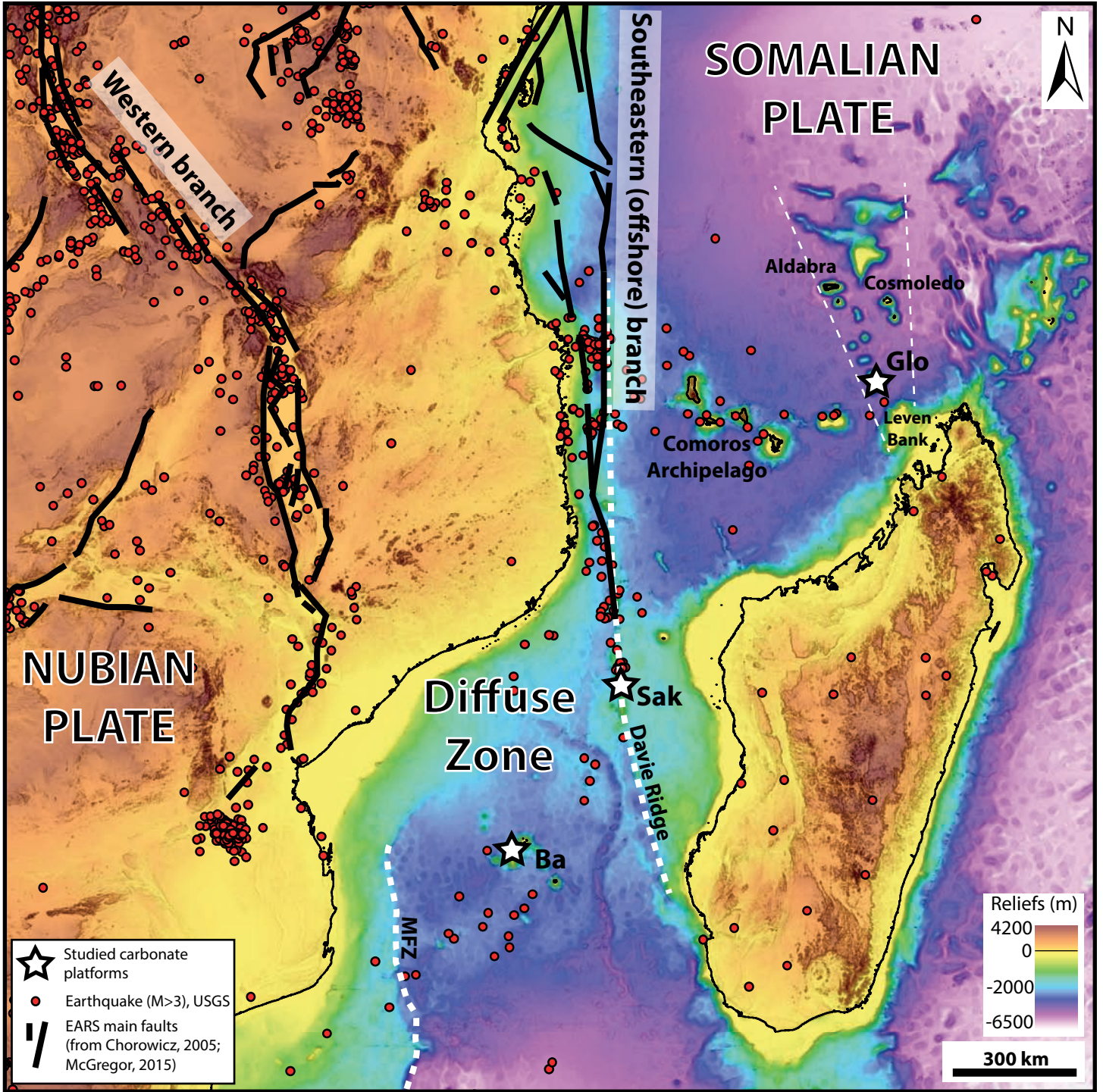
831 **Supplemental Data Captions**

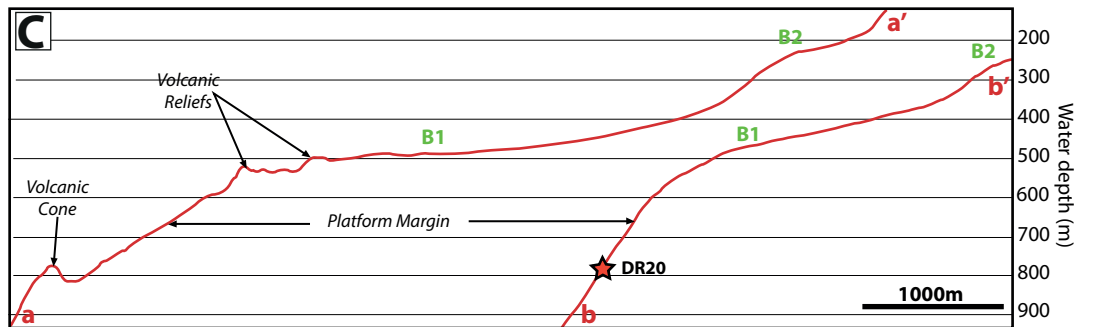
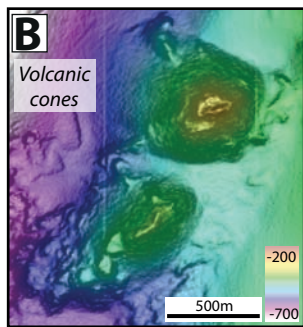
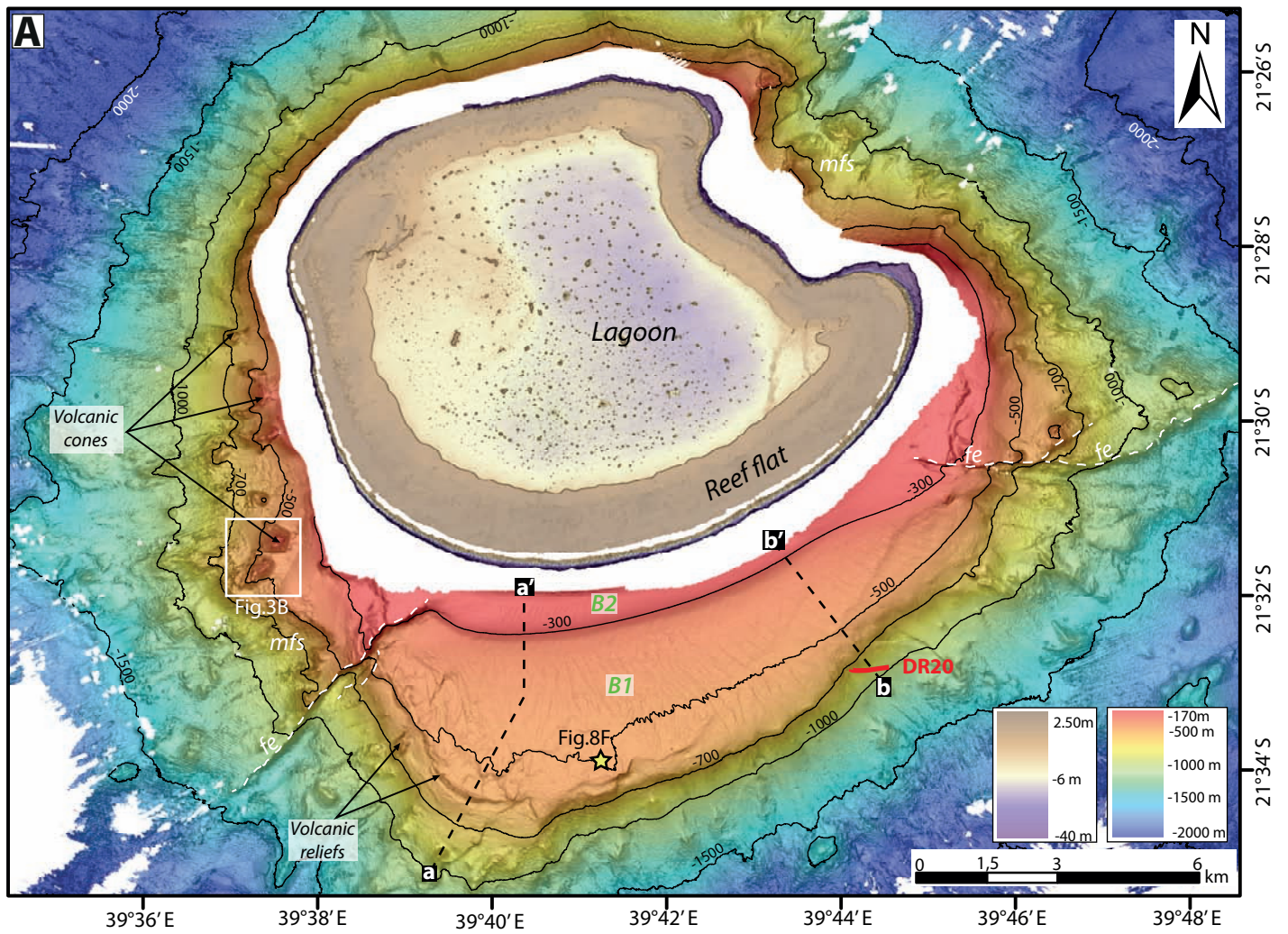
832 **Supplementary 1:** Synthetic tab about strontium isotopic stratigraphy (SIS) including  
833 SR87/SR86 ratios, ages and associated errors.

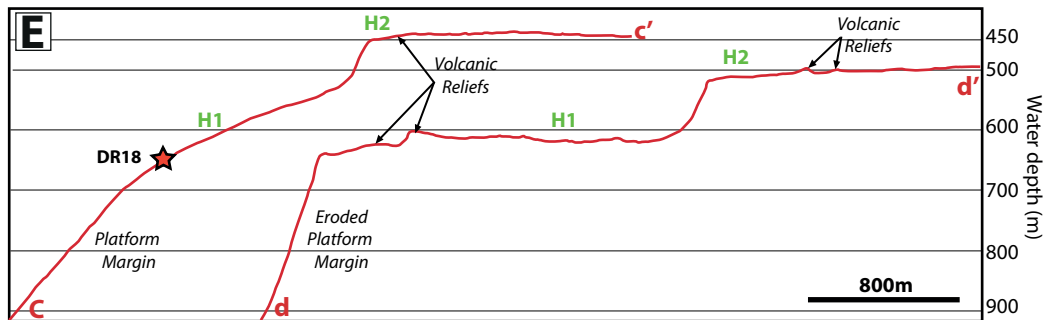
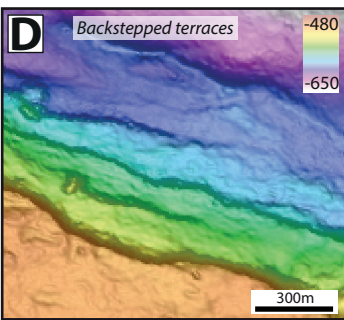
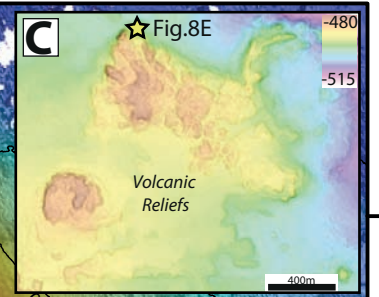
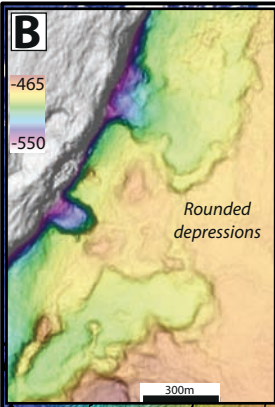
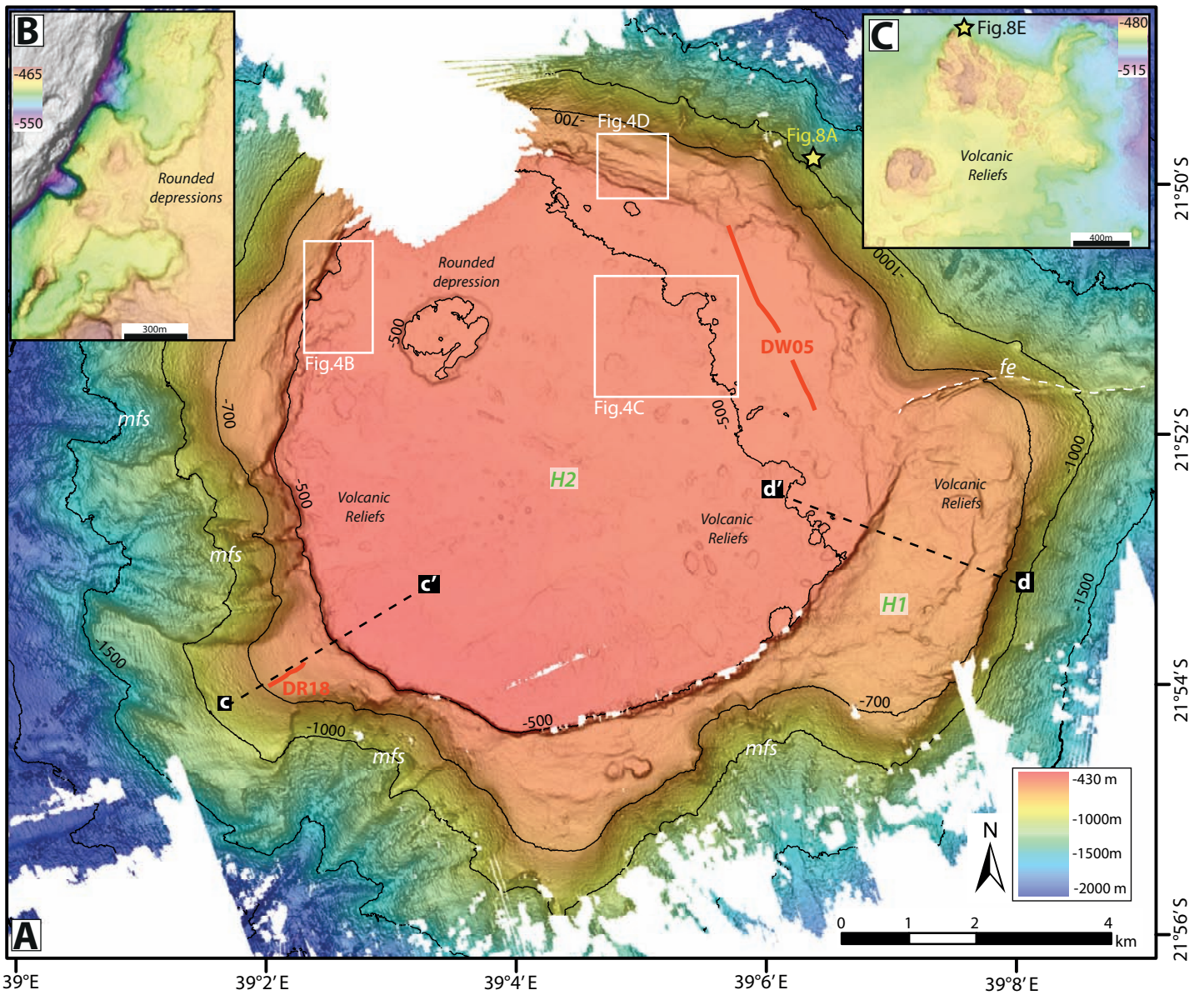
834 **Supplementary 2:** Volcanic rock samples collected along rough isolates ridges of the  
835 Mozambique Channel. DR17-05, DR19-03, DR13-01 & DW05-01: Alkali mafic lava  
836 fragments; DW05-01: heterogeneous volcanic breccia; DR04-22: trachy-andesite to trachyte  
837 lava block

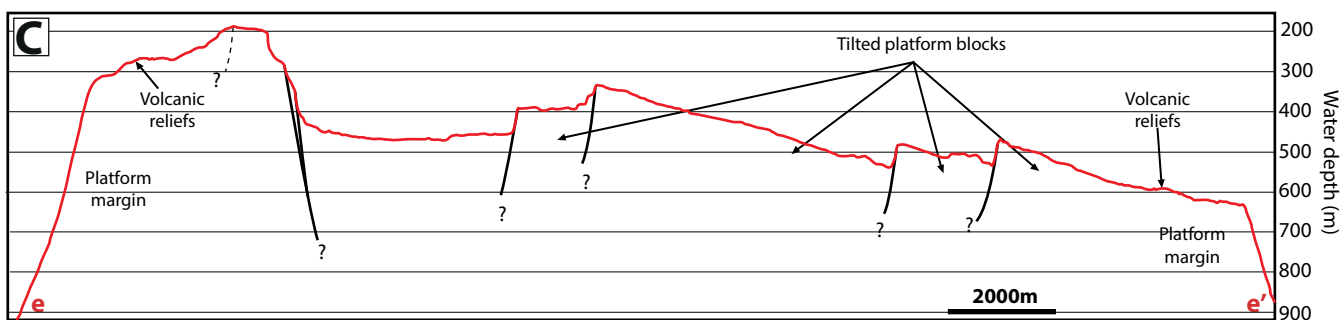
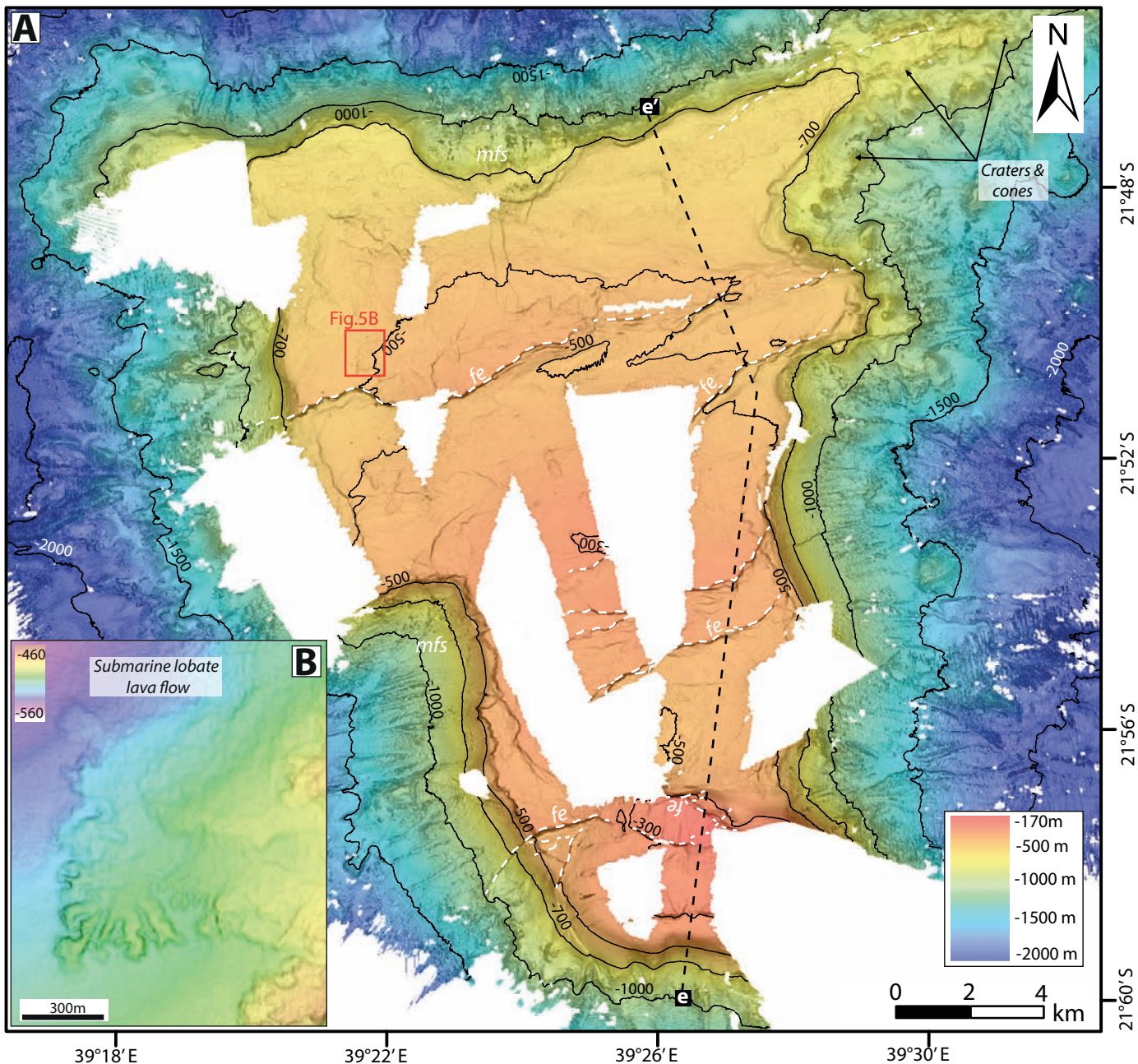
838

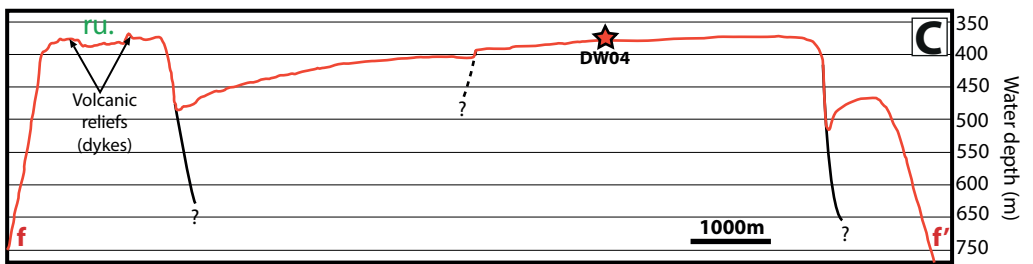
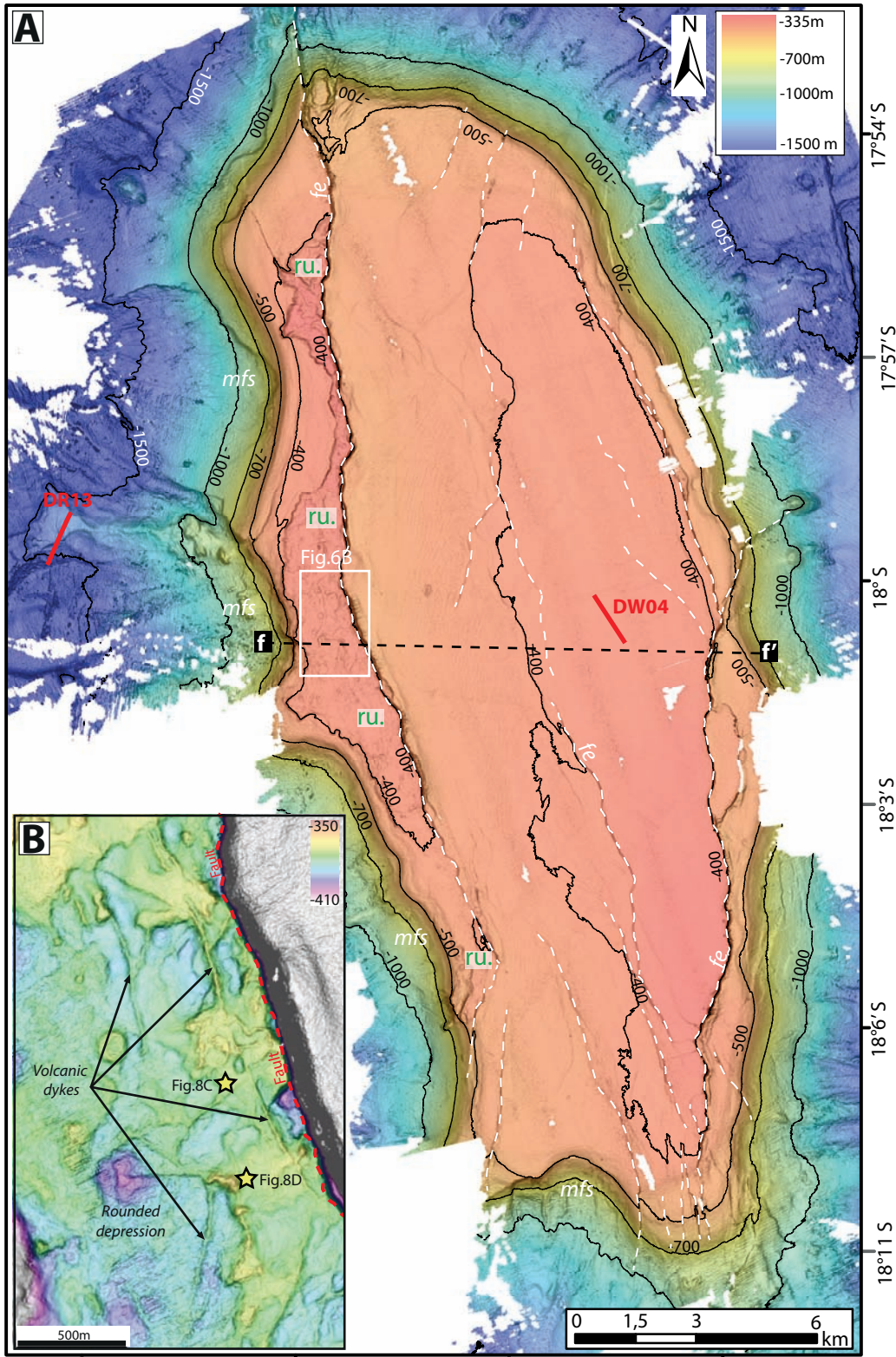


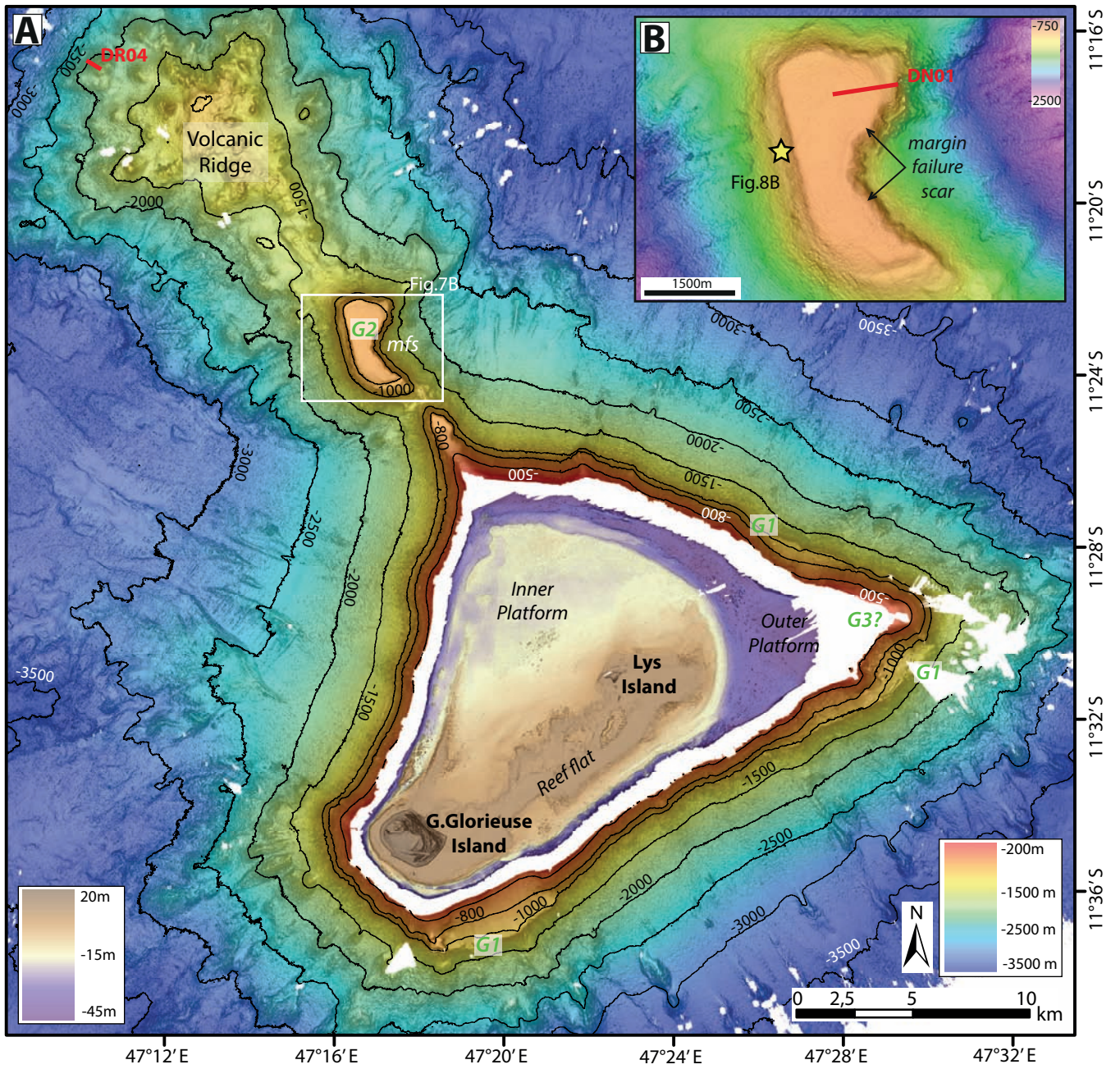


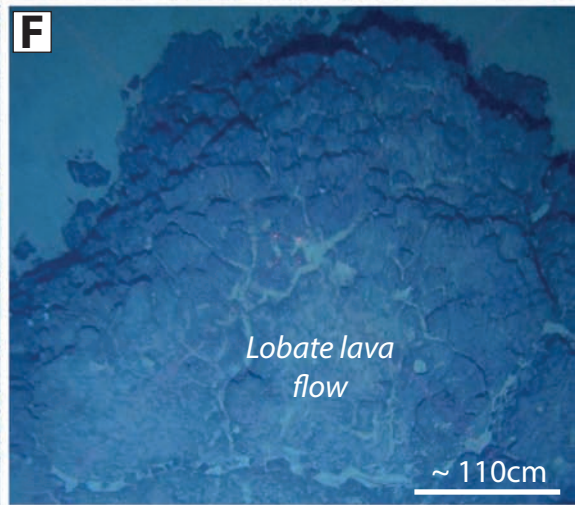
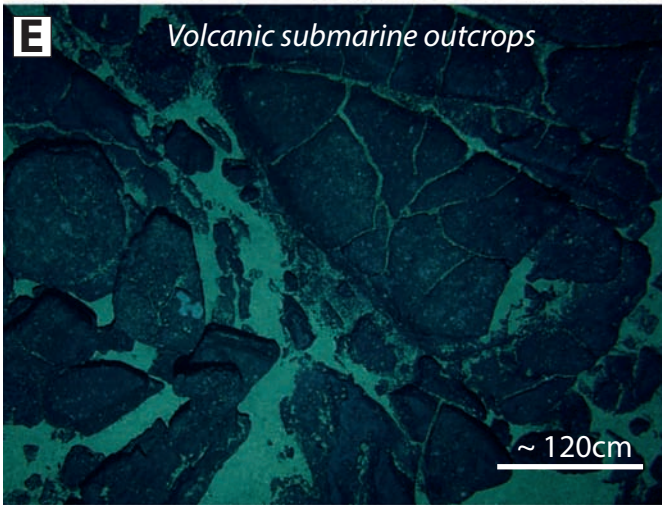
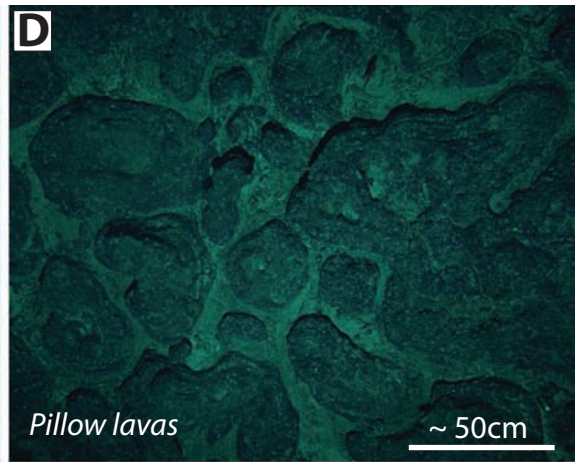
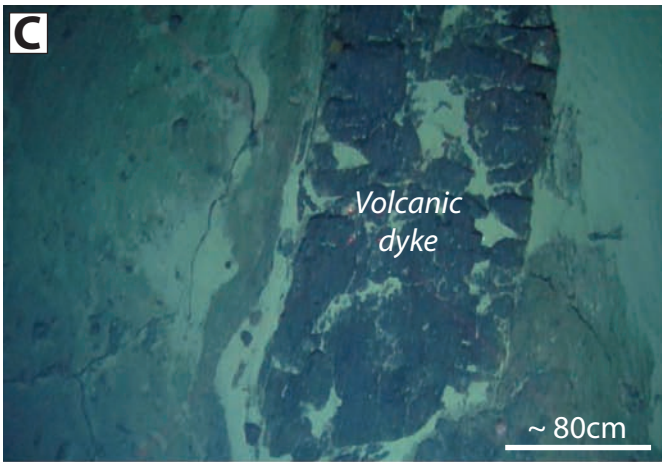
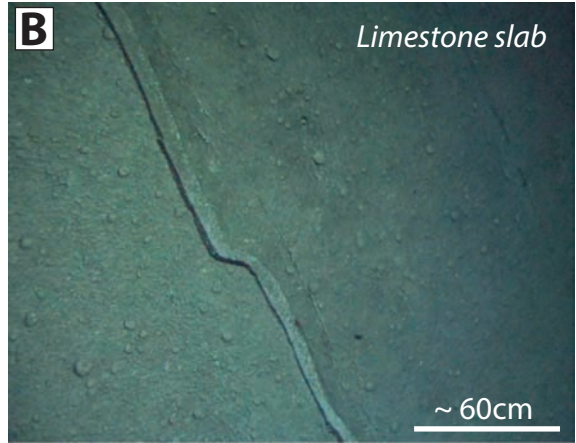


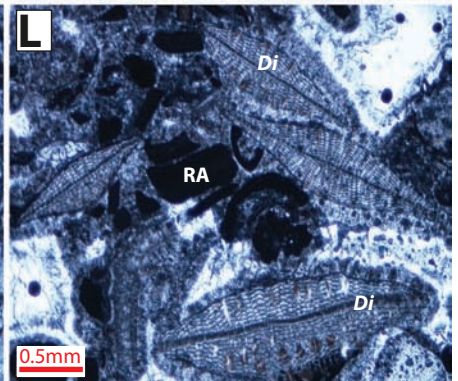
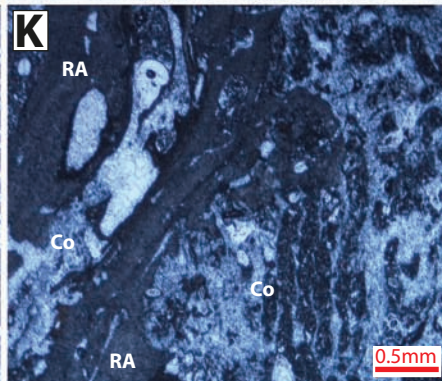
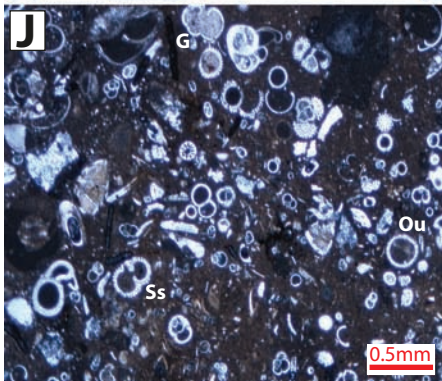
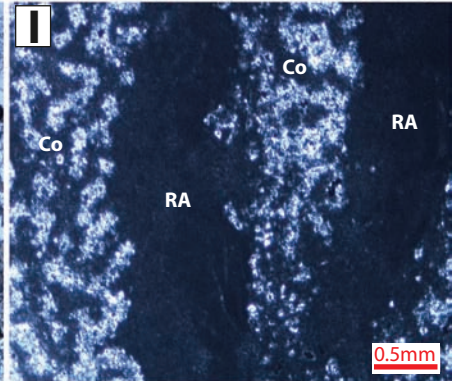
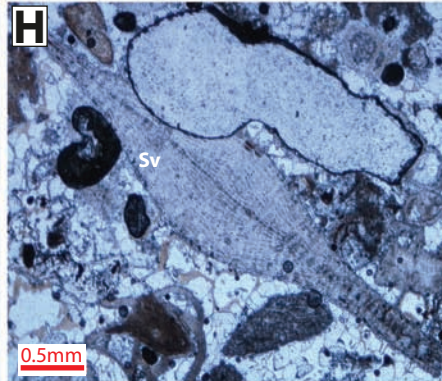
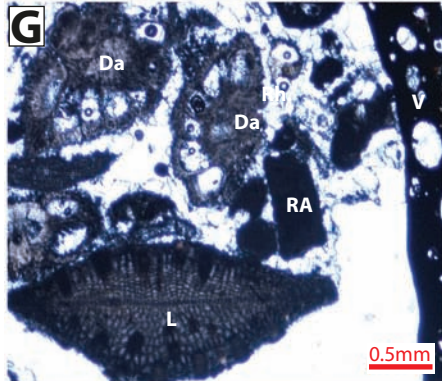
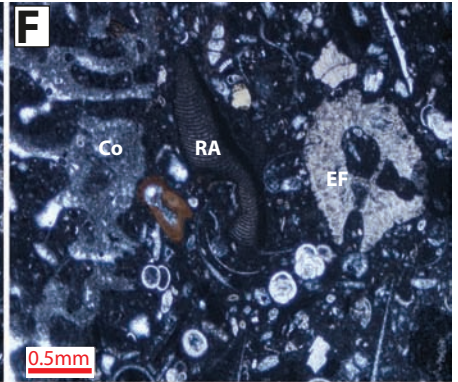
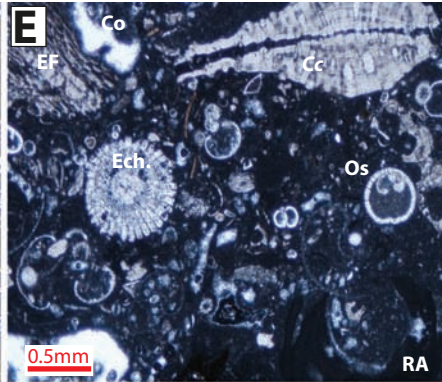
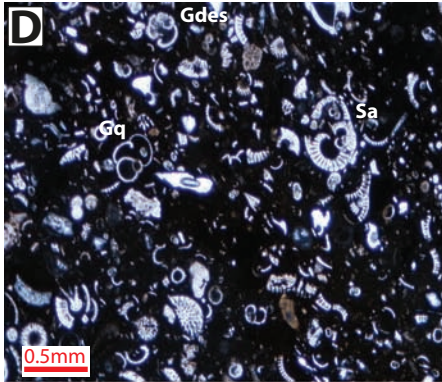
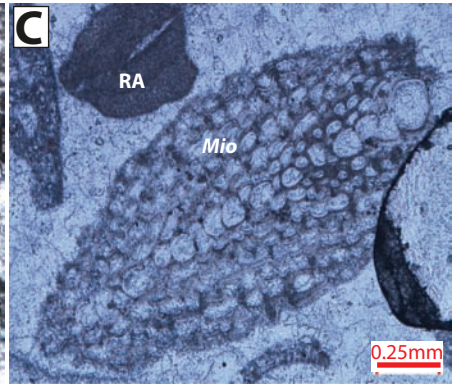
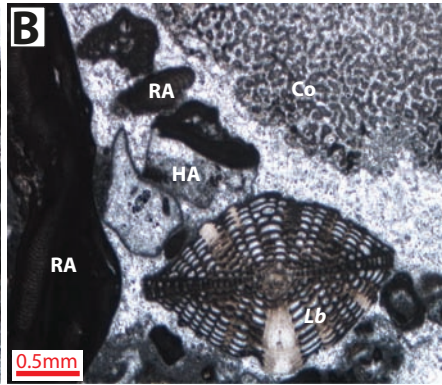
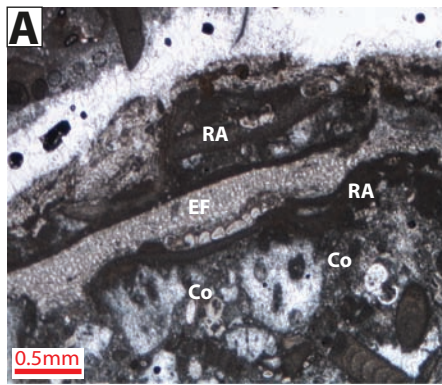






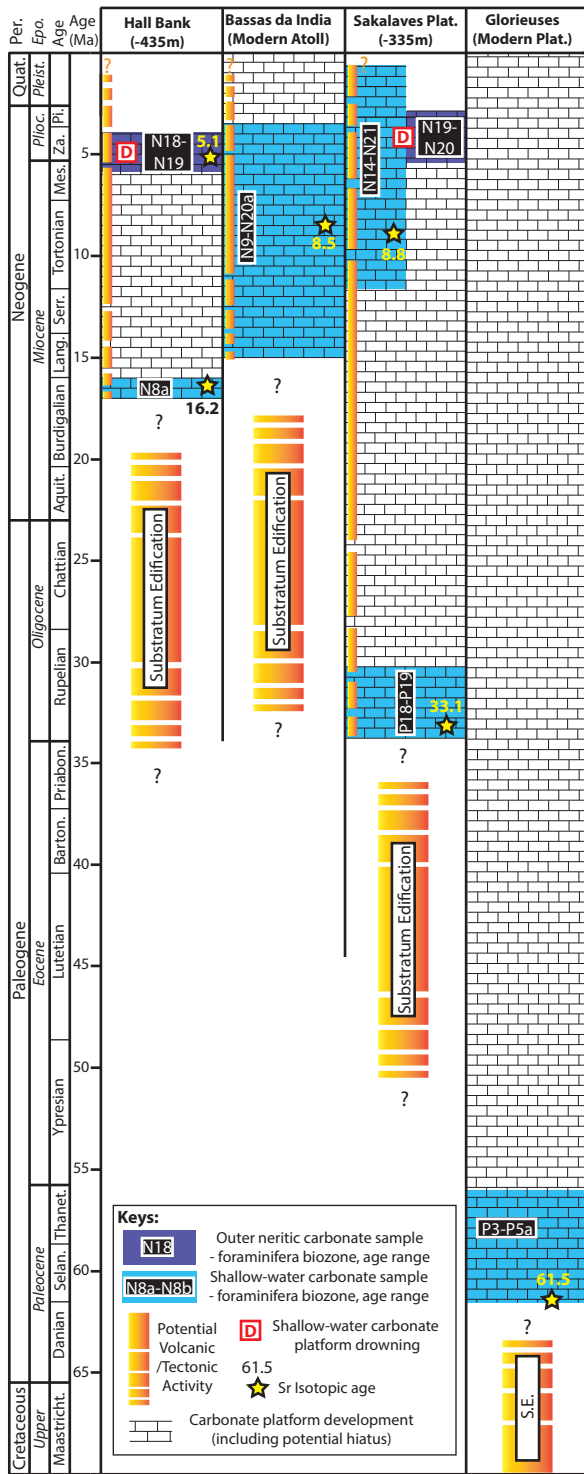






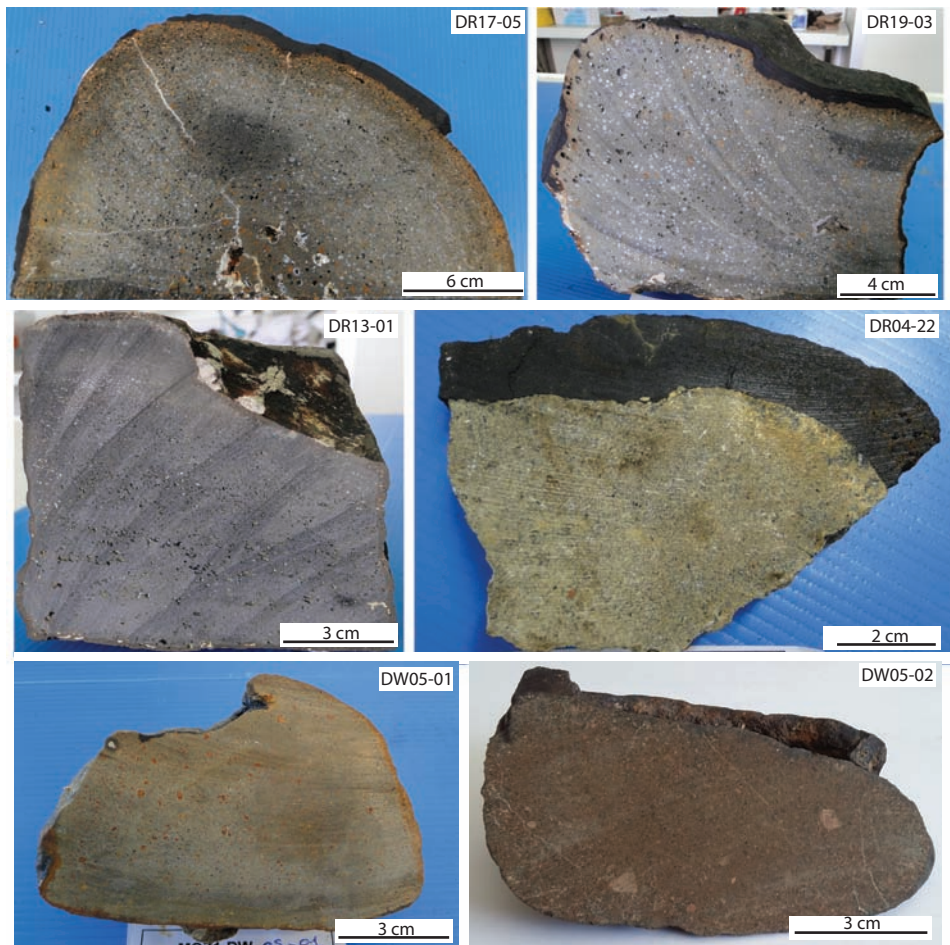
Site	Sample	Age based on Foraminifera first appearances. <i>Planktonic Foraminiferal zones, Shallow benthic zones and letter stages after BouDagher-Fadel (2008, 2013 &amp; 2015)</i>	Age based on Strontium Isotopic Stratigraphy (SIS) <i>Reference curve from McArthur (2012)</i>	Depositional Texture	Composition Major components (in order of abundance) <i>Minor components</i>	Depositional Environment
Hall Bank	DR18-01	N8a, 17-15.9 Ma, Burdigalian ( Early Miocene)	16.29 +/- 0.10 Ma, Burdigalian (Early Miocene)	Skeletal packstone with encrusted coral grains	Coral, Red Algae, LBF, <i>Halimeda</i> sp., EF <i>Echinoids, Bryozoans, Bivalves, Gastropods, PF</i>	Shallow-water tropical platform
	DW05-C1	N18-N19, 5.8 - 3.8 Ma, Late Messinian - Early Zanclean	5.09 +/- 0.08 Ma, Zanclean (Early Pliocene)	Packstone of planktonic foraminifera	PF <i>Echinoids, Bivalves, Gastropods</i>	Outer Neritic/Pelagic
Bassas da India	DR20-01	N9-N20a, 15.0 - 3.6 Ma, Middle Miocene - Early Pliocene	8.48 +/- 0.49 Ma, Tortonian (Late Miocene)	Skeletal packstone	PF, EF, Corals, Red Algae, LBF (some reworked forms), bivalves <i>Echinoids, Gastropods, Bryozoans, Halimeda sp.</i>	Shallow-water tropical platform
Sakalaves platform	D13-08	P18-P19, 33.9 - 30.3 Ma, Rupelian (Oligocene)	33.11 +/- 0.14 Ma, Rupelian (Oligocene)	Skeletal grainstone of LBF with rodolith fragments	LBF, Red algae, Volcanic fragments, EF <i>Bivalves, Echinoids, Gastropods, Bryozoans, Green algae</i>	Shallow-water tropical platform
	DW04-01	N14-N21 , 11.6 - 1 .6 Ma, Late Miocene- Pleistocene	8.80 +/- 0.35 Ma, Tortonian (Late Miocene)	Coralgal boundstone	Coral, Red algae <i>LBF, Gastropods</i>	Shallow-water tropical platform
	DW04-02a	N19-N20, 5.3 - 3.4 Ma, Zanclean (Early Pliocene)	No data	Packstone of planktonic foraminifera	PF <i>Bivalves, Echinoids, Gastropods, SBF</i>	Outer Neritic/Pelagic
Glorieuses	DN01-01	P3-P5a, 61.6 - 56.0 Ma, Selandian - Thanetian (Paleocene)	61.52 +/- 1.80 Ma*; Selandian (Paleocene)	Coralgal boundstone with pockets of LBF packstone	Red algae, LBF, Coral, EF <i>Bryozoans, Echinoids, Bivalves, Gastropods, SBF, PF</i>	Shallow-water tropical platform

\*(or 33.89 +/- 0.15 Ma or 67.11 +/- 0.27 Ma) LBF: Large Benthic Foraminifera; SBF: Small Benthic Foraminifera; EF: Encrusting Foraminifera; PF: Planktonic Foraminifera



Sample	$^{87}\text{Sr}/^{86}\text{Sr}$	1sigma error	Age (Ma)	+/- (Ma)
DR18-01	0.708702	0.000003	16.29	0.10
DW05-C1	0.709033	0.000005	5.09	0.08
DR20-01	0.708927	0.000003	8.48	0.49
D13-08	0.707856	0.000004	33.11	0.14
DW04-01	0.708921	0.000008	8.80	0.35
DN0-01	0.707812	0.000003	33.89	0.15
			61.52	1.80
			67.11	0.27

**Supplementary 1**



**Supplementary 2**